Geometric Continuity, Feb 08 2001

Jörg Peters[1* a]

[a]Dept C.I.S.E., CSE Bldg, University of Florida, Gainesville, FL 32611-6120, USA, e-mail: jorg@cise.ufl.edu, tel: US (352) 392-1226

This chapter covers geometric continuity with emphasis on a constructive definition for piecewise parametrized surfaces. The examples in Section 1 show the need for a notion of continuity different from the direct matching of Taylor expansions used to define the continuity of piecewise functions. Section 2 defines geometric continuity for parametric curves, and for surfaces, first along edges, then around points, and finally for a whole complex of patches which is called a G^k free-form surface spline. Here G^k characterizes a relation between specific maps while C^k continuity is a property of the resulting surface. The composition constraint on reparametrizations and the vertex-enclosure constraints are highlighted. Section 3 covers alternative definitions based on geometric invariants, global and regional reparametrization and briefly discusses geometric continuity in the context of implicit representations and generalized subdivision. Section 4 explains the generic construction of G^k free-form surface splines and points to some low degree constructions. The chapter closes with a listing of additional literature.

1. Motivating Examples

This section points out the difference between geometric continuity for curves and surfaces and the continuity for functions. The examples are formulated in the Bézier representation.

Two C^k function pieces join smoothly at a boundary to form a joint C^k function if, at all common points, their κth derivatives agree for $\kappa = 0, 1, \ldots, k$. Since the x, y and z components of curves and surfaces are functions, it is tempting to declare that curve or surface pieces join smoothly if and only if the derivatives of the component functions agree. However, as the following four examples illustrate, this criterion is neither sufficient nor necessary for characterizing smooth curves or smooth surfaces motivating the definitions in Section 2.

The first two examples illustrate the inadequacy of the standard notion of smoothness for functions when applied to *curves*. In Figure 1 the V of VC is parametrized by the two quadratic pieces, $u, v \in [0, 1]$,

$$\mathbf{q}_1(u) = \left[\begin{smallmatrix}-1\\1\end{smallmatrix}\right](1-u)^2 + \left[\begin{smallmatrix}0\\0\end{smallmatrix}\right]2(1-u)u + \left[\begin{smallmatrix}0\\0\end{smallmatrix}\right]u^2$$

and

$$\mathbf{q}_2(v) = \left[\begin{smallmatrix}0\\0\end{smallmatrix}\right](1-v)^2 + \left[\begin{smallmatrix}0\\0\end{smallmatrix}\right]2(1-v)v + \left[\begin{smallmatrix}1\\1\end{smallmatrix}\right]v^2.$$

*NSF NYI CCR-9457806

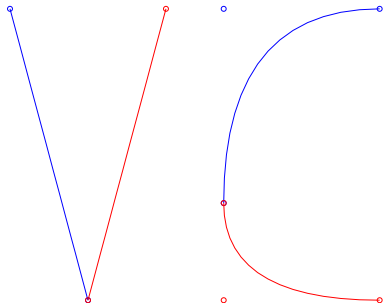

Figure 1. Matching derivatives of the component functions and geometric (visual) continuity are not the same: the V of VC is parametrized by two parabolic arcs with equal derivatives at the tip, but the V shape is not geometrically continuous; the C of VC is parametrized by two parabolic arcs with unequal derivatives at their common point, but the C shape is geometrically continuous.

Evidently, at the common point $\mathbf{q}_1(1) = \left[\begin{smallmatrix}0\\0\end{smallmatrix}\right] = \mathbf{q}_2(0)$ the derivatives agree:

$$(D\mathbf{q}_1)(1) = \left[\begin{smallmatrix}0\\0\end{smallmatrix}\right] = (D\mathbf{q}_2)(0).$$

However, even with suitably cushioned end points, the V should not be handed over to boys or girls under the age of 1 for fear of injury from the sharp corner. Matching derivatives clearly do not always imply smoothness. Conversely, smoothness does not imply matching derivatives. The C of VC is parametrized by the two quadratic pieces, $u, v \in [0, 1]$,

$$\mathbf{q}_3(u) = \left[\begin{smallmatrix}3\\2\end{smallmatrix}\right](1-u)^2 + \left[\begin{smallmatrix}0\\2\end{smallmatrix}\right]2(1-u)u + \left[\begin{smallmatrix}0\\0\end{smallmatrix}\right]u^2$$

and

$$\mathbf{q}_4(v) = \left[\begin{smallmatrix}0\\0\end{smallmatrix}\right](1-v)^2 + \left[\begin{smallmatrix}0\\-1\end{smallmatrix}\right]2(1-v)v + \left[\begin{smallmatrix}3\\-1\end{smallmatrix}\right]v^2.$$

The C is visually (and geometrically) smooth at the common point $\mathbf{q}_3(1) = \left[\begin{smallmatrix}0\\0\end{smallmatrix}\right]$ since the two pieces have the same vertical tangent line but the derivatives do not agree:

$$(D\mathbf{q}_3)(1) = \left[\begin{smallmatrix}0\\-4\end{smallmatrix}\right] \neq \left[\begin{smallmatrix}0\\-2\end{smallmatrix}\right] = (D\mathbf{q}_4)(0).$$

Both examples could be made consistent with our notion of continuity for functions if we ruled out parametrizations with zero derivative and substituted $v \to 2v$ in $\mathbf{q}_4$. In the case of *surfaces*, the distinction between higher-order continuity of the component functions and actual (geometric) continuity of the surface is more subtle.

In two variables, we contrast the smoothness criteria for surfaces with the concept valid for functions by looking at two examples involving polynomial pieces in total degree Bézier form, i.e. de Casteljau's triangles **??**. A necessary and sufficient geometric criterion for two polynomial pieces $p_1, p_2 : \mathbb{R}^2 \mapsto \mathbb{R}$ to join C^1 along a common boundary, is the 'coplanarity condition' **??**, illustrated in Figure 3,*left*; the function pieces p_1 and p_2 join C^1 if all subtriangles

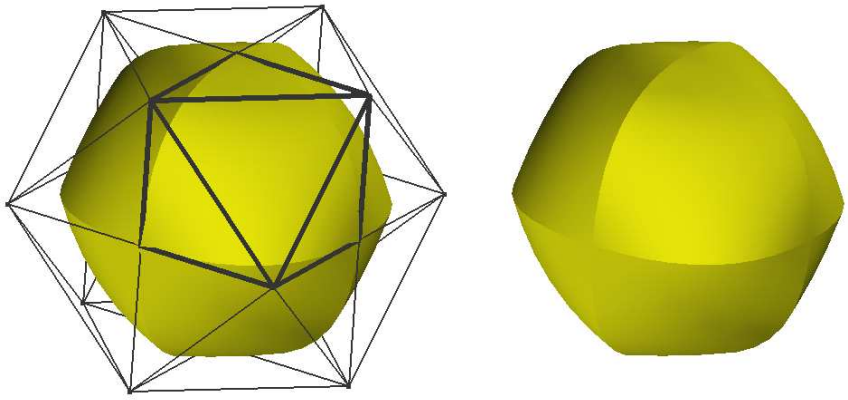

Figure 2. (*left*) The 6-point control net of one degree 2 patch in Bézier form is drawn in *thick lines*. The two subtriangles in the control net that include the end points of a boundary of the patch define the derivative along that boundary. For two edge-adjacent patches these subtriangles are mirror images and coplanar with their counterparts in the other patch. Still the surface defined by the patches is not tangent continuous as the creases in the surface demonstrate. (The creases are visible in the silhouette and in the change in surface shading, *right*).

of the control net that share two boundary points are coplanar. Since the coplanarity of the edge-adjacent triangles of the control net is a geometric criterion it is tempting to use it as a definition of smoothness for surfaces consisting of the 3-sided patches. However, the criterion is neither sufficient nor necessary.

To see that coplanarity of the edge-adjacent triangles of the control net does not imply tangent continuity of the surface consider the eight degree 2 triangular polynomial patches whose control nets are obtained by chopping off the eight corners of a cube down to the midpoint of each edge (Figure 2). The edge midpoints and face centers of the cube serve as the control points of 8 quadratic 3-sided Bézier patches. For example, the patch in the positive octant (with thick control lines in Figure 2, *left*) has the coefficients

$$\begin{bmatrix} 0 \\ 1 \\ 0 \end{bmatrix} \quad \begin{bmatrix} 0 \\ 1 \\ 1 \end{bmatrix} \quad \begin{bmatrix} 0 \\ 0 \\ 1 \end{bmatrix} \quad \begin{bmatrix} 1 \\ 1 \\ 0 \end{bmatrix} \quad \begin{bmatrix} 1 \\ 0 \\ 1 \end{bmatrix} \quad \begin{bmatrix} 1 \\ 0 \\ 0 \end{bmatrix}$$

Figure 2, *right* shows that the patches join with a sharp crease at the middle of their common parabolic boundaries. Indeed, the normal at the midpoint $\begin{bmatrix} .75 \\ .75 \\ 0 \end{bmatrix}$ of the equatorial boundary of the positive octant patch is $\begin{bmatrix} 2/3 \\ 2/3 \\ 1/3 \end{bmatrix}$, but to match its counterpart in the lower hemisphere, by symmetry, the z-component would have to be zero. Upper and lower hemisphere therefore do not meet with a continuous normal.

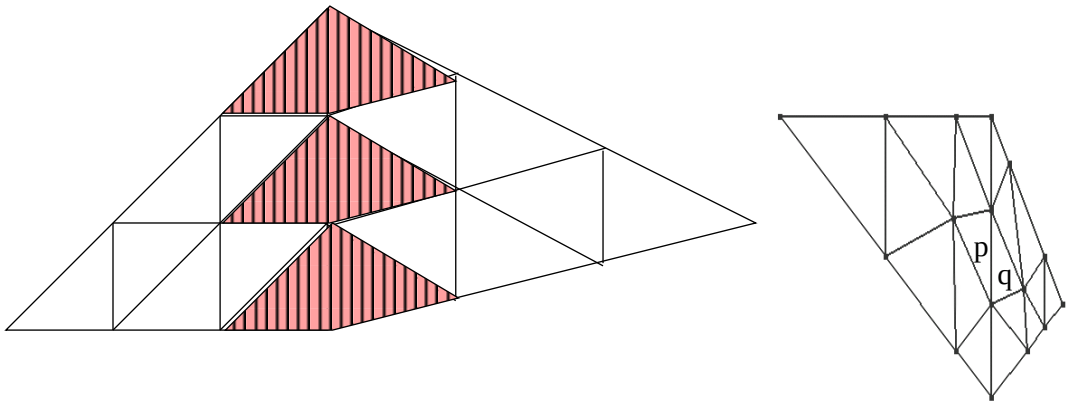

Figure 3. (*left*) Two function pieces p_1 and p_2 join C^1 if all subtriangles of the control net that share two boundary points (*striped*) are coplanar (Farin's C^1 condition). (*right*) Even though the middle cross-boundary subtriangle pair (where the patch labels $\mathbf{p}$ and $\mathbf{q}$ are placed, *right*) are *not* coplanar the two Bézier patches $\mathbf{p}(\Delta)$ and $\mathbf{q}(\Delta)$ join to form a tangent continuous surface.

Conversely, the geometric coplanarity criterion is not necessary for a smooth join. The two cubic pieces $\mathbf{p}, \mathbf{q}$ with coefficients (c.f. Figure 3)

$$\mathbf{p}: \begin{bmatrix} 72 \\ 72 \\ 6 \end{bmatrix} \begin{bmatrix} 36 \\ 36 \\ 0 \end{bmatrix} \begin{bmatrix} 72 \\ 36 \\ 12 \end{bmatrix} \begin{bmatrix} 12 \\ 12 \\ 0 \end{bmatrix} \begin{bmatrix} 46 \\ 13 \\ 0 \end{bmatrix} \begin{bmatrix} 72 \\ 12 \\ 12 \end{bmatrix} \begin{bmatrix} 0 \\ 0 \\ 0 \end{bmatrix} \begin{bmatrix} 24 \\ 0 \\ 0 \end{bmatrix} \begin{bmatrix} 48 \\ 0 \\ 12 \end{bmatrix} \begin{bmatrix} 72 \\ 0 \\ 12 \end{bmatrix}$$

$$\mathbf{q}: \begin{bmatrix} 0 \\ 0 \\ 0 \end{bmatrix} \begin{bmatrix} 24 \\ 0 \\ 0 \end{bmatrix} \begin{bmatrix} 48 \\ 0 \\ 12 \end{bmatrix} \begin{bmatrix} 72 \\ 0 \\ 12 \end{bmatrix} \begin{bmatrix} 12 \\ -12 \\ 0 \end{bmatrix} \begin{bmatrix} 28 \\ -11 \\ 12 \end{bmatrix} \begin{bmatrix} 60 \\ -6 \\ 12 \end{bmatrix} \begin{bmatrix} 18 \\ -18 \\ 0 \end{bmatrix} \begin{bmatrix} 36 \\ -18 \\ 12 \end{bmatrix} \begin{bmatrix} 24 \\ -24 \\ 6 \end{bmatrix}$$

have the partial derivatives $D_1\mathbf{p}$ and $D_2\mathbf{q}$ along and $D_2\mathbf{p}$, respectively $D_1\mathbf{q}$ across the common boundary:

$$\begin{aligned}
(D_1\mathbf{p})(t,0) &= \begin{bmatrix} 72 \\ 0 \\ 0 \end{bmatrix} (1-t)^2 + \begin{bmatrix} 72 \\ 0 \\ 36 \end{bmatrix} 2(1-t)t + \begin{bmatrix} 72 \\ 0 \\ 0 \end{bmatrix} t^2 = (D_2\mathbf{q})(0,t), \\
(D_2\mathbf{p})(t,0) &= \begin{bmatrix} 36 \\ 36 \\ 0 \end{bmatrix} (1-t)^2 + \begin{bmatrix} 66 \\ 39 \\ 0 \end{bmatrix} 2(1-t)t + \begin{bmatrix} 72 \\ 36 \\ 0 \end{bmatrix} t^2, \\
(D_1\mathbf{q})(0,t) &= \begin{bmatrix} 36 \\ -36 \\ 0 \end{bmatrix} (1-t)^2 + \begin{bmatrix} 12 \\ -33 \\ 36 \end{bmatrix} 2(1-t)t + \begin{bmatrix} 36 \\ -18 \\ 0 \end{bmatrix} t^2.
\end{aligned}$$

With the help of Maple we can check that the partial derivatives are coplanar at every point of the boundary, i.e. $\det\big(D_1\mathbf{p}(t,0), D_2\mathbf{p}(t,0), D_1\mathbf{q}(0,t)\big) = 0$, the zero polynomial in t. Since

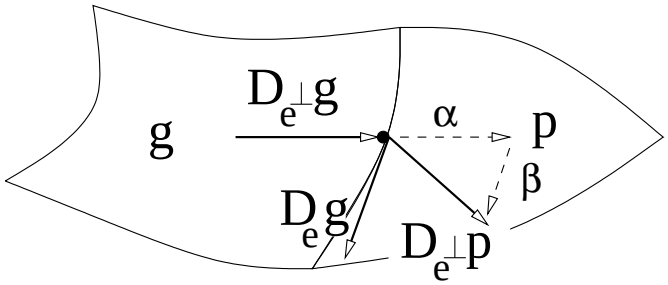

Figure 4. If the patches meet with tangent continuity, the transversal derivative $D_{e^\perp}\mathbf{p}$ of $\mathbf{p}$ must be a linear combination of the versal derivative vector $D_e\mathbf{g}$ in the direction e along the preimage E of common boundary $\mathbf{p}(E)$ and the transversal derivative $D_{e^\perp}\mathbf{g}$ in the direction $e^\perp$ perpendicular to e: $D_{e^\perp}\mathbf{p} = \alpha D_e\mathbf{g} + \beta D_{e^\perp}\mathbf{g}$.

the surface pieces neither form a cusp nor have vanishing derivatives along the boundary, the normal direction varies continuously across. Maple also yields

$$\det(\begin{bmatrix}72\\0\\36\end{bmatrix}, \begin{bmatrix}66\\39\\0\end{bmatrix}, \begin{bmatrix}12\\-33\\36\end{bmatrix}) = 5832 \neq 0$$

showing that, in contrast to a C^1 match between two functions, edge-adjacent subtriangle pairs need not each be coplanar.

1.1. Differentiation and Evaluation

Even though derivatives of the component functions by themselves do not yield a correct picture of curve and surface continuity, the definition of geometric continuity relies on derivatives. And since we work with functions in several variables, some clarification of notation is in order.

First, it is at times clearer to denote evaluation at a point Q by $f\mid_Q$ rather than $f(Q)$, evaluation on points along a curve segment E by $f\mid_E$ and to use the symbol $\circ$ for composition, i.e. $\mathbf{g}\circ\mathbf{r} = \mathbf{g}(\mathbf{r})$. We use bold font for vector-valued functions but, somewhat inconsistently but ink-saving, regular font for directions of differentiation e and points of evaluation, say Q or 0, the zero vector in $\mathbb{R}^n$. The notation D^κ for the κth derivative in one variable is consistent with the notation in two variables from [102]:

Definition 1.1 (differentiation) *The differentials $D^\kappa\mathbf{p}$ of a map $\mathbf{p}:\mathbb{R}^2\mapsto\mathbb{R}^3$ with x-, y- and z-components $\mathbf{p}^{[x]}$, $\mathbf{p}^{[y]}$, $\mathbf{p}^{[z]}$ and the domain spanned by the unit vectors $e_1\perp e_2$ are defined recursively as*

$$D_{e_i}\mathbf{p}^{[x]}\mid_Q := \lim_{t\downarrow 0}\frac{\mathbf{p}^{[x]}(Q+te_i)-\mathbf{p}^{[x]}(Q)}{t},\quad D_{e_1}\mathbf{p} := \begin{bmatrix}D_{e_1}\mathbf{p}^{[x]}\\D_{e_1}\mathbf{p}^{[y]}\\D_{e_1}\mathbf{p}^{[z]}\end{bmatrix},\quad D\mathbf{p} := \begin{bmatrix}D_{e_1}\mathbf{p} & D_{e_2}\mathbf{p}\end{bmatrix},$$

$$D^\kappa := DD^{\kappa-1},\ \textit{e.g.}\ D^2\mathbf{p} = DD\mathbf{p} = \begin{bmatrix}D_{e_1}D_{e_1}\mathbf{p} & D_{e_2}D_{e_1}\mathbf{p}\\D_{e_1}D_{e_2}\mathbf{p} & D_{e_2}D_{e_2}\mathbf{p}\end{bmatrix}.$$

If the Jacobian $D\mathbf{p}$ is of full rank 2, $\mathbf{p}$ is called regular. *We abbreviate $D_ip = D_{e_i}p$.*

In *one variable* (see e.g. [17])

$$D^\kappa(\mathbf{g}\circ\rho)=\sum_{j=0}^{\kappa}\sum_{K(j)}c_{K(j)}\Big((D^j\mathbf{g})\circ\rho\Big)\cdot(D^1\rho)^{k_1}\cdot\ldots\cdot(D^\kappa\rho)^{k_\kappa}.$$

This combination of the chain rule and the product rule is called *Faá di Bruno's Law* and the bookkeeping is hidden in the index set

$$K(j):=\{k_i\geq 0, i=1,\ldots,\kappa,\ \sum_{i=1}^{\kappa}k_i=j,\ \sum_{i=1}^{\kappa}ik_i=\kappa\},\ c_{K(j)}:=\frac{\kappa!}{k_1!(1!)^{k_1}\cdots k_\kappa!(\kappa!)^{k_\kappa}},$$

In two variables $D^\kappa\mathbf{g}$ (no subscript) is a κ-linear map acting on $\mathbb{R}^{2\times\kappa}$ (κ terms). Its component with index $(i_1,i_2,\ldots,i_\kappa)\in\{1,2\}^\kappa$ is $D_{i_1}D_{i_2}\cdots D_{i_\kappa}\mathbf{g}$. The arguments of $D^\kappa\mathbf{g}$ are surrounded by $\langle\cdot\rangle$ and $\langle\mathbf{a},\mathbf{a},\ldots,\mathbf{a},\mathbf{b},\ldots,\mathbf{b}\rangle$ with $\mathbf{a}\in\mathbb{R}^2$ repeated i times and $\mathbf{b}\in\mathbb{R}^2$ repeated j times is abbreviated as $\langle(\mathbf{a})^i,(\mathbf{b})^j\rangle$. We can then write the bivariate *Faá di Bruno's Law* as

$$D_1^\kappa(\mathbf{g}\circ\mathbf{r})=\sum_{j=0}^{\kappa}\sum_{K(j)}c_{K(j)}\Big((D^j\mathbf{g})\circ\mathbf{r}\Big)\langle(D_1^1\mathbf{r})^{k_1},\ldots,(D_1^\kappa\mathbf{r})^{k_\kappa}\rangle.$$

For example

$$\begin{aligned}D^2f\langle\mathbf{a},\mathbf{b}\rangle&=\begin{bmatrix}\mathbf{a}^{[1]} & \mathbf{a}^{[2]}\end{bmatrix}\begin{bmatrix}D_1^2f & D_1D_2f\\ D_1D_2f & D_2^2f\end{bmatrix}\begin{bmatrix}\mathbf{b}^{[1]}\\ \mathbf{b}^{[2]}\end{bmatrix}\\&=\mathbf{a}^{[1]}\mathbf{b}^{[1]}D_1^2f+(\mathbf{a}^{[1]}\mathbf{b}^{[2]}+\mathbf{a}^{[2]}\mathbf{b}^{[1]})D_1D_2f+\mathbf{a}^{[2]}\mathbf{b}^{[2]}D_2^2f.\end{aligned}$$

2. Geometric Continuity of Parametric Curves and Surfaces

This section defines kth order geometric continuity, short G^k continuity, as agreement of derivatives after suitable reparametrization, i.e. paraphrasing [57], 'geometric continuity is a relaxation of parametrization, and not a relaxation of smoothness'. Section 3 will show that G^1 and G^2 are equivalent notions to tangent and curvature continuity.

2.1. Joining Parametric Curve Pieces

Definition 2.1 (G^k join) *Two C^k curve segments* $\mathbf{q}$ *and* $\mathbf{p}$ join at $\mathbf{p}(0)$ with geometric continuity G^k via the C^k map $\rho:\mathbb{R}\mapsto\mathbb{R}$ *if*

$$D^\kappa(\mathbf{g}\circ\rho)\mid_0=D^\kappa\mathbf{p}\mid_0\quad\kappa=0,\ldots,k,\qquad D\rho\mid_0>0, D\mathbf{p}\mid_0\neq 0.$$

The map ρ is called reparametrization. *If $\rho=$* id*, the identity map, then* $\mathbf{p}$ *and* $\mathbf{g}$ *are said to join* parametrically C^k.

The contraint $D\rho\mid_0>0$ rules out cusps and other singularities.

With the abbreviation $\mathbf{j}^k\mathbf{p}\mid_0=[\mathbf{p}\mid_0,D\mathbf{p}\mid_0,\ldots,D^k\mathbf{p}\mid_0]^T\in\mathbb{R}^{(k+1)\times n}$ for $\mathbf{p}\in\mathbb{R}^n$ Fáa di Bruno's law can be written as

$$\mathbf{j}^k\mathbf{p}\mid_0=\mathbf{A}(\mathbf{j}^k\mathbf{g})\mid_{\rho(0)},\qquad\mathbf{A}=\begin{bmatrix}1 & & & & & \\ D\rho & & & & & \\ D^2\rho & (D\rho)^2 & & & & \\ D^3\rho & \alpha & (D\rho)^3 & & & \\ \vdots & \vdots & \vdots & \ddots & & \\ D^k\rho & \ldots & \ldots & \ldots & (D\rho)^k\end{bmatrix}\mid_0,\quad\alpha=3D\rho D^2\rho.$$

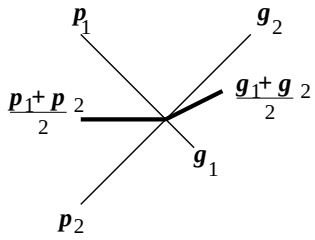

Figure 5. The average (*bold* lines) of two curves whose pieces $\mathbf{p}_i$ and $\mathbf{g}_i$ join G^∞ can be tangent discontinuous, i.e. its pieces do not even join G^1.

The matrix of derivatives of ρ is called G^k *connection matrix* [13], [109] or β-matrix [7] and $\mathbf{j}^k\mathbf{p}$ is the k-*jet* of $\mathbf{p}$. In one variable, two regular maps $\mathbf{p}$ and $\mathbf{q}$ can both be reparametrized so that $\mathbf{p}(\rho_\mathbf{p})$ and $\mathbf{q}(\rho_\mathbf{q})$ have the preferred *arclength parametrization* **??** , i.e. unit increments in the parameter correspond to unit increments in the length of the curve. Then $\mathbf{j}^k(\mathbf{p}\circ\rho_\mathbf{p})\mid_0 = \mathbf{j}^k(\mathbf{q}\circ\rho_\mathbf{q})\mid_0$.

G^k splines with different connection matrices do not form a common vector space; in particular the average of two curves that join G^k is not necessarily G^k as illustrated in Figure 5: if $\mathbf{p}_1$ and $\mathbf{q}_1$ join G^k via ρ_1 at $\mathbf{p}_1(0)$ and $\mathbf{p}_2$ and $\mathbf{q}_2$ join G^k via ρ_2 at $\mathbf{p}_2(0)=\mathbf{p}_1(0)$ then, in general, there does not exist a reparametrization ρ so that $(1-\sigma)\mathbf{p}_1+\sigma\mathbf{p}_2$ joins G^k with $(1-\sigma)\mathbf{g}_1+\sigma\mathbf{g}_2$ at $\mathbf{p}_2(0)=\mathbf{p}_1(0)$. That is, there does not generally exist a connection matrix A such that

$$A_1(1-\sigma)\mathbf{j}^k\mathbf{g}_1 + A_2\sigma\mathbf{j}^k\mathbf{g}_2 = A((1-\sigma)\mathbf{j}^k\mathbf{g}_1+\sigma\mathbf{j}^k\mathbf{g}_2).$$

In the example shown in Figure 5, $\mathbf{j}^1\mathbf{p}_1 = \left[\begin{smallmatrix}0 & 1\\ 0 & -1\end{smallmatrix}\right]$, $\mathbf{j}^1\mathbf{g}_1 = \left[\begin{smallmatrix}0 & 1\\ 0 & -1/3\end{smallmatrix}\right]$, $A_1 = \left[\begin{smallmatrix}1 & 0\\ 0 & 3\end{smallmatrix}\right]$, and $\mathbf{j}^1\mathbf{g}_2 = \mathbf{j}^1\mathbf{p}_2 = \left[\begin{smallmatrix}0 & 1\\ 0 & 1\end{smallmatrix}\right]$, but $\mathbf{j}^1(\mathbf{p}_1+\mathbf{p}_2)/2 = \left[\begin{smallmatrix}0 & 1\\ 0 & 0\end{smallmatrix}\right]$ while $\mathbf{j}^1(\mathbf{g}_1+\mathbf{g}_2)/2 = \left[\begin{smallmatrix}0 & 2/3\\ 0 & 1/3\end{smallmatrix}\right]$ and there does not exist a G^1 connection matrix $A = \left[\begin{smallmatrix}1 & 0\\ 0 & D\rho\end{smallmatrix}\right]$ such that $\mathbf{j}^1(\mathbf{p}_1+\mathbf{p}_2)/2 = A\mathbf{j}^1(\mathbf{g}_1+\mathbf{g}_2)/2$.

However, if we *fix* a $(\kappa_i+1)\times(\kappa_i+1)$ connection matrix at the ith breakpoint, we can construct a space of degree k splines with prescribed G^{κ_i} joints and knots of order $k-\kappa_i$. Such a spline space can be analyzed as the affine image of a 'universal spline' whose control points are in general position [109].

Conversely, any given polygon can be interpreted as the control polygon of a G^k spline: by interated linear interpolation the polygon is refined into one whose vertices, when interpreted as Bézier coefficients, define curve pieces that join G^k, e.g. [11] for $k=2$, [37] for Frénet frame continuity (see Section 3.1) and [109], [110], [111] for the general case.

There are *degree-optimal constructions* for this conversion, i.e. constructions that maximise the smoothness of the spline for a given number of corner cuts that translate into polynomial degree. Via the notion of order of contact (see Section 3.1) smoothness is closely related to the ability to interpolate, say the data of a previous spline segment. Following the pioneering paper [19] where it was observed that a cubic segment can often interpolate position, tangent and curvature at either end point (see also [63],[21]), Koch and Höllig [60] conjectured that,

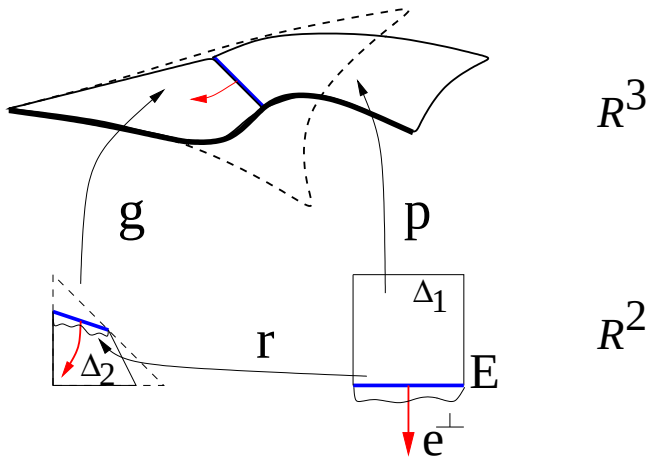

Figure 6. Reparametrization $\mathbf{r} : \mathbb{R}^2 \mapsto \mathbb{R}^2$ and geometry maps $\mathbf{p}, \mathbf{g} : \mathbb{R}^2 \mapsto \mathbb{R}^3$. For a G^k join via $\mathbf{r}$ the traversal derivatives $D^\kappa_{e^\perp}(\mathbf{g} \circ \mathbf{r})$ and $D^\kappa_{e^\perp}\mathbf{p}$ have to agree along the common boundary $\mathbf{p}(E)$ for $\kappa = 0, \ldots, k$. The dashed lines indicate that $\mathbf{r}(E)$ need not be a boundary edge of the domain of $\mathbf{g}$.

under suitable assumptions, "splines of degree $\leq n$ can interpolate points on a smooth curve in $\mathbb{R}^m$ with order of contact $k - 1 = n - 1 + \lfloor (n-1)/(m-1) \rfloor$ at every n^{th} knot. Moreover, this geometric Hermite interpolant has the optimal approximation order $k + 1$" (see also [97]). CHECK

2.2. Geometric Continuity of Edge-Adjacent Patches

We now turn to a constructive characterization of the smoothness of *surfaces* assembled from standard pieces used in CAGD, such as 3- or 4-sided Bézier patches, or tensor-product b-spline patches.

Definition 2.2 (domain, reparametrization, geometry map, patch)

- *A* domain *is a closed subset* Δ *of* $\mathbb{R}^2$*, bounded by a finite number of* edges E.
- *Let* Δ_1 *and* Δ_2 *be domains. A* C^k reparametrization *is a* C^k *continuous invertible map* $\mathbf{r} : \mathbb{R}^2 \mapsto \mathbb{R}^2$*, defined in a neighborhood of an edge* E *of* Δ_1 *and mapping exterior points of* Δ_1 *to interior points of* Δ_2.
- *A* C^k geometry map *is a map* $\mathbf{g} : \Delta \mapsto \mathbb{R}^3$ *such that* $D^\kappa \mathbf{g}, \kappa = 0, \ldots, k$ *is continuous and* $\det(D\mathbf{g}) \neq 0$*;* $\mathbf{g}(\Delta)$ *is a* C^k patch.

The requirement that geometry map be regular, i.e. $\det(D\mathbf{g}) \neq 0$, rules out geometric singularities, such as cones, cusps or ridges, and avoids special cases – but it off-hand also rules out singular maps that generate perfectly smooth surfaces ([81], [76], [15], [98]). These constructions are shown to be smooth by a local change of variable that removes the singularity.

Defining the domain boundary to consist of a few edges is specific to CAGD usage: we could have a fractal boundary separating two pieces of the same smooth surface.

The map $\mathbf{g}$ is called geometry map to emphasize that the local shape (but not the extent) of the surface is defined by $\mathbf{g}$. The image of $\mathbf{g}$ in $\mathbb{R}^3$ is the patch.

The reparametrization $\mathbf{r}$ is not defined to map E to a *boundary edge* of Δ_2 but may map to any non-selfintersecting curve segment $\mathbf{r}(E)$ in Δ_2. This allows for constructions that include trimmed geometry maps, as indicated by the restriction of the triangular domain of $\mathbf{g}$ in Figure 6. That is, $\mathbf{r}$ not only modifies the flow of parameter lines (images of straight lines in the domain) but it can also restrict the region of evaluation of $\mathbf{g}$. The reparametrization $\mathbf{r}$ maps outside points to inside points to prevent the surface from folding back onto itself in a $180°$-turn. We now glue two pieces together (c.f. Figure 6).

Definition 2.3 (G^k join) *Two C^k geometry maps* $\mathbf{p}$ *and* $\mathbf{g}$ join along $\mathbf{p}(E)$ with geometric continuity G^k via the C^k reparametrization $\mathbf{r}$ *if*

$$D^\kappa \mathbf{p} \mid_E = D^\kappa(\mathbf{g} \circ \mathbf{r}) \mid_E, \quad \kappa = 0, \ldots, k.$$

If $\mathbf{r} = \mathrm{id}$*, the identity map, then* $\mathbf{p}$ *and* $\mathbf{g}$ *are said to join* parametrically C^k.

Since $\mathbf{p}$, $\mathbf{g}$ and $\mathbf{r}$ are C^k maps, G^k continuity along $\mathbf{p}(E)$ with C^k reparametrization $\mathbf{r}$ is equivalent to just $k+1$ equalities corresponding to differentiation in the direction $e^\perp$ perpendicular to the edge E:

$$D^\kappa_{e^\perp} \mathbf{p} \mid_E = D^\kappa_{e^\perp}(\mathbf{g} \circ \mathbf{r}) \mid_E, \quad \kappa = 0, \ldots, k.$$

By Faá di Bruno's Law we need only know the Taylor expansion up to kth order of $\mathbf{r}$ and $\mathbf{g}$ along the edge E.

Example Consider two C^2 geometry maps $\mathbf{p}$ and $\mathbf{g}$, and a C^2 reparametrization $\mathbf{r} : \mathbf{r}(t,0) = (0,t)$. As shown in Figure 6, $E = \{(t,0) : t \in [0,1]\}$ and $e^\perp = (0,-1)$. A less common, but permissible parametrization of E is $\{(t^2,0) : t \in [0,1]\}$. Such a definition would make the subtle point that G^0 and C^0 can differ as well, since the reparametrization $\mathbf{r}(t,0) = (0,\sqrt{t})$ is required to equate the derivatives along the boundary. (If $\mathbf{p}$ and $\mathbf{g}$ are polynomials of the same least degree then $\mathbf{r}$ can only be linear and $\mathbf{p}$ and $\mathbf{g}$ share the same parametrization along the edge). We write the conditions for $\mathbf{p}$ and $\mathbf{g}$ joining G^2 via $\mathbf{r}$ along $\mathbf{p}(E)$ in several different notations commonly used in the literature, e.g. the mixed partial derivative may be written as $\mathbf{g}_{uv} = \frac{\partial^2 \mathbf{g}}{\partial u \partial v} = \partial_{12}\mathbf{g} = D_{12}\mathbf{g} = D_{e_1,e_2}\mathbf{g}$.

$$\begin{aligned}
\mathbf{p} \mid_{(t,0)} &= \mathbf{g} \circ \mathbf{r} \mid_{(t,0)}, \\
D_{e^\perp}\mathbf{p} \mid_{(t,0)} &= D\mathbf{g} \mid_{\mathbf{r}(t,0)} \cdot (D_{e^\perp}\mathbf{r}) \mid_{(t,0)} \\
&= D_{e_1}\mathbf{g} \mid_{(0,t)} (D_{e^\perp}\mathbf{r})^{[1]} \mid_{(t,0)} + D_{e_2}\mathbf{g} \mid_{(0,t)} (D_{e^\perp}\mathbf{r})^{[2]} \mid_{(t,0)}, \quad (D_{e^\perp}\mathbf{r})^{[2]} > 0, \\
&= \mathbf{g}_u(0,t)\alpha(t) + \mathbf{g}_v(0,t)\beta(t), \quad \beta > 0, \\
D^2_{e^\perp}\mathbf{p} \mid_{(t,0)} &= (D^2\mathbf{g} \mid_{\mathbf{r}(t,0)})\langle (D_{e^\perp}\mathbf{r}) \mid_{(t,0)}, (D_{e^\perp}\mathbf{r}) \mid_{(t,0)} \rangle + D\mathbf{g} \mid_{\mathbf{r}(t,0)} D^2_{e^\perp}\mathbf{r} \mid_{(t,0)} \\
&= \ldots + D_2\mathbf{g} \mid_{(0,t)} (D^2_{e^\perp}\mathbf{r})^{[2]} \mid_{(t,0)} \\
&= \mathbf{g}_{uu}(0,t)\alpha^2(t) + 2\mathbf{g}_{uv}(0,t)\alpha(t)\beta(t) + \mathbf{g}_{vv}(0,t)\beta^2(t) \\
&\quad + \mathbf{g}_u(0,t)\sigma(t) + \mathbf{g}_v(0,t)\tau(t).
\end{aligned}$$

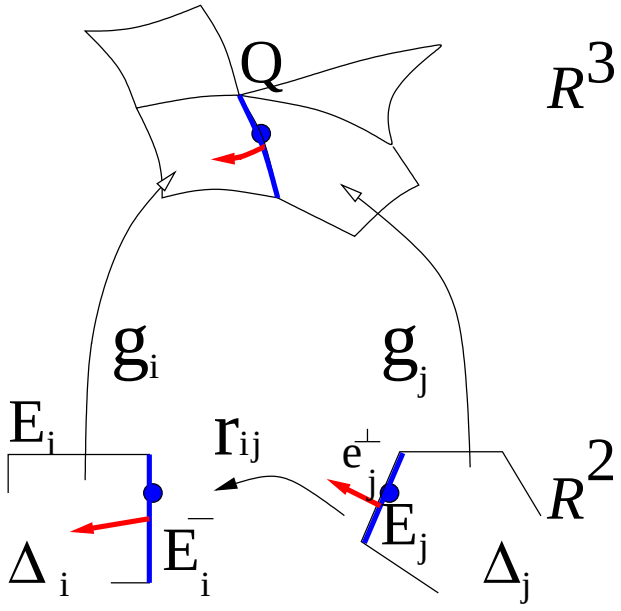

Figure 7. Patches meeting at a corner $Q = \mathbf{g}_i(E_i(0))$, $j = (i \mod n) + 1$; $E_i(0) = E_i^-(1)$.

In particular for $\mathbf{p}$ and $\mathbf{q}$ defined on page 4 we compute $D_{e_1}\mathbf{q}\,|_{(t,0)} = D\mathbf{p}\,|_{(t,0)} \cdot \begin{bmatrix} 1 \\ \frac{3-2u}{3-u} \end{bmatrix}$.

The example illustrates that it is convenient and shorter to give separate names, $\alpha, \beta, \sigma, \tau$, to the partial derivatives of $\mathbf{r}$ evaluated on the edge E. We can in fact specify just the partial derivatives rather than all of $\mathbf{r}$: if we group the two components of each derivative into a vector we can define $\mathbf{r}$ in terms of C^{k-j}-vector fields along $\mathbf{r}(E)$ (Lemma 3.2 of [52]). Provided the derivatives are sufficiently differentiable in the direction $e^{\perp}$ perpendicular to E we thereby prescribe the Taylor expansion of $\mathbf{r}$ (by the Whitney-Stein Theorem).

2.3. Geometric Continuity at a Vertex

We extend our new notion of geometric continuity to $\mathtt{n}$ patches meeting at a common point, e.g. at a point of the global boundary where the patches may meet without necessarily enclosing the point (c.f. Figure 7).

Definition 2.4 (G^k enclosure) *The C^k geometry maps $\mathbf{g}_i : \Delta_i \mapsto \mathbb{R}^3, i = 1, \ldots, \mathtt{n}$,* meet G^k via $\mathbf{r}_{i,i+1}, i = 1, \ldots, \mathtt{n}-1$ with corner $Q \in \mathbb{R}^3$ *if*

- $\mathbf{g}_i$ *and* $\mathbf{g}_{i+1}$ *join G^k via* $\mathbf{r}_{i,i+1}$ *along* $\mathbf{g}_{i+1}(E_{i+1})$,
- $\mathbf{g}_i(E_i(0)) = Q$,
- *the normalized tangent vectors of each* $\mathbf{g}_i$ *sweep out a sector of a disk and these* tangent sectors *lie in a common plane and do not overlap.*

The C^k geometry maps form a G^k enclosure of the vertex Q *if additionally* $\mathbf{g}_{\mathtt{n}}$ *and* $\mathbf{g}_1$ *join G^k via* $\mathbf{r}_{\mathtt{n},1}$ *along* $\mathbf{g}_1(E_1)$.

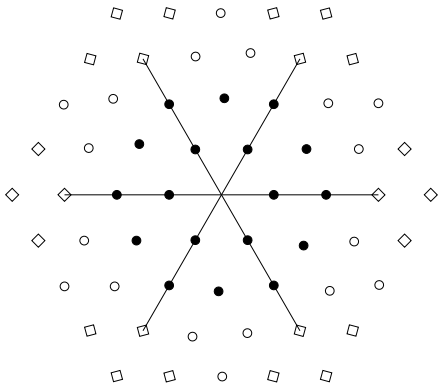

Figure 8. The derivative $D_1^m D_2^n \mathbf{p}_i$ of a geometry map $\mathbf{p}_i$ at the central vertex is represented symbolically as a $\bullet$, $\circ$, or $\diamond$ placed m units into the direction of the first edge and n into the second. Elements of the total-degree 2-jet $\mathbf{j}^2$ are marked $\bullet$, elements of the coordinate-degree 2-jet $\mathbf{J}^2$ are marked $\bullet$ or $\circ$, elements of $\mathbf{j}^4$ are marked $\bullet$, $\circ$, or $\diamond$. The higher-order derivatives H_i^k appearing on the right hand side of the vertex-enclosure constraint system are marked by diamonds $\diamond$.

The regularity of the C^k geometry maps implies that each tangent sector is the 1 to 1 image of a corner formed by the non-collinear edges E^- and E of the domain. Moreover, the geometry maps do not wrap around the corner more than once. The common plane referred to above is therefore the tangent plane and, by the implicit function theorem we can expand the geometry maps at Q as a C^k functions.

Where a point is *enclosed* by three or more patches, additional constraints on $\mathbf{r}$ and $\mathbf{g}$ arise because patches join in a cycle. If one were to start with one patch and added one patch at a time, the last patch would have to match pairwise smoothness constraints across two of its edges. More generally, if all patches are determined simultaneously, a circular interdependence among the smoothness constraints around the vertex results. This circular dependence implies *composition constraints* on admissible $\mathbf{r}$ and *vertex enclosure constraints*, on the $\mathbf{g}_i$. The latter imply for example the important practical fact that it is not always possible to interpolate a given *network of C^1 curves* by a smooth, regularly parametrized tangent-plane continuous surface with one polynomial patch per mesh facet [82]. A characterization, of when a curve network can be embedded into a curvature continuous surface can be found in [53].

To discuss the details, the k-jet notation (c.f. page 7) is helpful:

Definition 2.5 *The* coordinate-degree k-jet, $\mathbf{J}^k\mathbf{p}$, *is a vector of directional derivatives $D_1^i D_2^j \mathbf{p}$, $i, j \in \{0, 1, \ldots, k\}$ sorted first with key $i+j$, then with key i.The* total-degree k-jet, $\mathbf{j}^k\mathbf{p}$, *consists of the first $\binom{k}{2}$ entries of the coordinate-degree k-jet.*

For example, as illustrated in Figure 8 (see also [58], p.61, [52]),

$$\mathbf{j}^2\mathbf{p} := (\mathbf{p}, D_1\mathbf{p}, D_2\mathbf{p}, D_1^2\mathbf{p}, D_1D_2\mathbf{p}, D_2^2\mathbf{p}),$$
$$\mathbf{J}^2\mathbf{p} := (\mathbf{p}, D_1\mathbf{p}, D_2\mathbf{p}, D_1^2\mathbf{p}, D_1D_2\mathbf{p}, D_2^2\mathbf{p}, D_1^2D_2\mathbf{p}, D_1D_2^2\mathbf{p}, D_1^2D_2^2\mathbf{p}).$$

The composition of k-jets, $\mathbf{j}^k\mathbf{g}\mid_{\mathbf{r}(E)} \circ \mathbf{j}^k\mathbf{r}\mid_E = \mathbf{j}^k(\mathbf{g}\circ\mathbf{r})\mid_E$, is associative and has the identity map id as its neutral element. In k-jet notation the conditions for geometric continuity are

$$\mathbf{j}^k\mathbf{p}\mid_E = \mathbf{j}^k\mathbf{g}\mid_{\mathbf{r}(E)} \circ \mathbf{j}^k\mathbf{r}\mid_E.$$

2.3.1. Composition Constraint on Reparametrization Maps

Assume that $\mathbf{r}_{i,i+1}(0) = 0$, $0 \in \mathbb{R}$. Since $\mathbf{g}_1$ is regular, by the implicit function theorem $D\mathbf{g}_1$ has a left inverse in the neighborhood of 0 and

$$\begin{aligned}\mathbf{j}^k\mathbf{g}_1\mid_0 &= \mathbf{j}^k(\mathbf{g}_n\circ\mathbf{r}_{n,1})\mid_0 = \ldots = \mathbf{j}^k(\mathbf{g}_2\circ\mathbf{r}_{2,3}\circ\ldots\circ\mathbf{r}_{n,1})\mid_0\\ &= \mathbf{j}^k(\mathbf{g}_1\circ\mathbf{r}_{1,2}\circ\ldots\circ\mathbf{r}_{n,1})\mid_0\end{aligned}$$

implies that at 0 the Taylor expansion up to kth order of the composition of all reparametrizations agrees with the identity, i.e. the Composition Constraint

$$\mathbf{j}^k(\mathbf{r}_{1,2}\circ\ldots\circ\mathbf{r}_{n,1})\mid_0 = \mathbf{j}^k\mathrm{id}\mid_0.$$

Example For $k = 1$ and $n = 3$ and with $\mathbf{r}_{i,j}(0,t) = (t,0)$ we have

$$\begin{aligned}\mathbf{r}_{1,2}\circ\mathbf{r}_{2,3}\circ\mathbf{r}_{3,1}\mid_0 &= 0,\\ D\mathbf{r}_{1,2}D\mathbf{r}_{2,3}D\mathbf{r}_{3,1}\mid_0 &= D\,\mathrm{id}\mid_0.\end{aligned}$$

For scalars λ and μ, the second equation is equivalent to the matrix product

$$\begin{bmatrix}\lambda_1 & 1\\ \mu_1 & 0\end{bmatrix}\begin{bmatrix}\lambda_2 & 1\\ \mu_2 & 0\end{bmatrix}\begin{bmatrix}\lambda_3 & 1\\ \mu_3 & 0\end{bmatrix} = \begin{bmatrix}1 & 0\\ 0 & 1\end{bmatrix}$$

which is in turn equivalent to

$$\mu_1\mu_2\mu_3 = -1, \qquad \lambda_j\mu_i = 1, \quad i = 1,2,3, j = (i \mod 3) + 1.$$

In general, the G^1 constraints at 0 imply $\prod_{i=1}^{\mathtt{n}}\mu_i = (-1)^{\mathtt{n}}$. Section 7.2 of [52] shows the expansion of the nonlinear constraints for $k = 2$. ◇

Lemma 2.1 *A* symmetric *reparametrization* $\mathbf{r}_{ij} = \mathbf{r}$ *that satisfies the Composition Constraint for a given* $\mathtt{n}$ *is defined by*

$$\mathbf{r}(0) = 0, \quad D\mathbf{r} = \left[\begin{smallmatrix}2\cos(\alpha) & 1\\ -1 & 0\end{smallmatrix}\right], \quad \alpha = \frac{2\pi}{\mathtt{n}}, \quad D^\kappa\mathbf{r} = 0, \kappa > 1.$$

Proof The eigenvalues of $D\mathbf{r}$ are the $\mathtt{n}$ th unit roots $e^{\pm\sqrt{-1}\alpha}$ and therefore $D\mathbf{r}_{1,2}D\mathbf{r}_{2,3}\ldots D\mathbf{r}_{n,1} = (D\mathbf{r})^{\mathtt{n}} = D\mathrm{id}$. Since, by Fáa di Bruno's law, at least one factor of the expansion of $D^\kappa(\mathbf{r}_{1,2}\circ\mathbf{r}_{2,3}\circ\ldots\circ\mathbf{r}_{\mathtt{n},1})$ is a higher derivative of $\mathbf{r}$ and hence $D^\kappa(\mathbf{r}_{1,2}\circ\mathbf{r}_{2,3}\circ\ldots\circ\mathbf{r}_{\mathtt{n},1}) = 0, \quad$ for $\kappa > 1$. ⋈

2.3.2. Vertex Enclosure Constraints

Once the reparametrizations satisfy the Composition Constraint a second set of constraints governs admissible choices of geometry maps. Since the G^k constraints of two edge-adjacent patches have support on the first k layers of derivatives counting from each edge, the constraints across two consecutive edges of a geometry map share as variables the derivatives $D_1^m D_2^n$ with $m \leq k$ and $n \leq k$ at the vertex, i.e. overlap on the coordinate-degree k-jet of the geometry map at the vertex (markers $\bullet$ and $\circ$ in Figure 8).

If $\mathtt{n}$ is the number of patches surrounding the vertex, then there are $\mathtt{n}(k+1)^2$ overlapping continuity constraints and an equal number of variables in the form of derivatives in the corresponding coordinate degree k-jets $\mathbf{J}^k\mathbf{p}_i$. Can the constraints can always be enforced by choosing $\mathbf{J}^k\mathbf{p}_i$ appropriately? Already for $k = 1$, the resulting $4\mathtt{n}$ by $4\mathtt{n}$ constraint matrix $\mathcal{M}$ is not invertible if $\mathtt{n}$ is even but it is invertible for $\mathtt{n}$ odd. For $k > 1$, more complex rank-deficiences arise while the right hand side is in general not in the span of the constraint matrix: unlike the univariate case, where we consider only the first k derivatives for G^k joins, the G^k *vertex-enclosure constraints involve derivatives of up to order* $2k$!

Depending on the data and the construction scheme, some of the higher derivatives are fixed. For example, prescribing boundary curves pins down $D_1^i D_2^0 \mathbf{p}$ for all i. Even when the goal is to just identify degrees of freedom of a free-form spline space [36],[64], the underlying splines must have consistent derivatives up to order $2k$. There is one well-studied exceptional case: if the corner Q is the intersection of two regular C^k curves and $\mathtt{n} = 4$ then the constraint system becomes homogeneous, removing the linkage between the k-jets and the higher derivatives. Since the constraint matrix is additionally rank deficient it is possible to interpolate the curve data by low-degree, parametrically C^k surfaces [40], [39]. The corresponding free-form splines form the space of tensor-product splines [18].

When the reparametrizations are linear as in Lemma 2.1 then determining the matrix rank is similar to determining the *dimension of a spline space* [2], however with the additional requirement that the 'minimal determining set' $D_1^m D_2^n \mathbf{p}_i$ be symmetric. The analysis of the dimension of spline spaces allows choosing one geometry map completely and then finding extensions that respect the continuity constraints. This misses the crucial rank deficiencies that depend on the parity of k and $\mathtt{n}$.

The vertex-enclosure constraint is weaker than the *compatibility constraint*, e.g. the *twist compatibility* constraint requires that the mixed derivatives be prescribed consistently since $D_1 D_2 \mathbf{p} = D_2 D_1 \mathbf{p}$ holds for a polynomial finite element (see e.g. [4]). Mixed derivatives at a vertex can be prescribed inconsistently if a patch is to interpolate given transversal derivatives along abutting edges. Incompatibility can be accomodated by using poles or singular parametrizations (see page 4,(2), 3rd and 4th item).

The main task ahead is to characterize the rank deficiencies of the $\mathtt{n}(k+1)^2 \times \mathtt{n}(k+1)^2$ matrix $\mathcal{M}$ of the G^k constraint system

$$D_1^m D_2^n (\mathbf{p}_{i-1} - \mathbf{p}_i \circ \mathbf{r}_i) \mid_0 = 0 \quad \text{for } n, m \in \{0, \ldots, k\}, i = 1, \ldots, \mathtt{n}$$

in the variables $D_1^m D_2^n \mathbf{p}_i \mid_0, n, m \in \{0, \ldots, k\}, i = 1, \ldots, \mathtt{n}$. In terms of k-jets and $H_i^k := (D_1^{k+m} D_2^l \mathbf{p}_i)_{m=1,\ldots,k, l=0,\ldots,k-m}$, the vector of higher derivatives of $\mathbf{p}_i$, for example, $H_i^2 :=$

$(D_1^3\mathbf{p}_i, D_1^3D_2\mathbf{p}_i, D_1^4\mathbf{p}_i)$, the constraint system reads (all blank entries are zero)

$$\mathcal{M}\begin{bmatrix}\vdots\\ \mathbf{J}^k\mathbf{p}_i\\ \vdots\end{bmatrix} = \begin{bmatrix}\vdots\\ N_iH_i^k\\ \vdots\end{bmatrix}, \qquad \mathcal{M} := \begin{bmatrix} I & -M_2 & & & & \\ & I & -M_3 & & & \\ & & I & -M_4 & & \\ & & & \ddots & \ddots & \\ & & & & I & -M_{\mathtt{n}} \\ -M_1 & & & & & I \end{bmatrix}$$

$$M_i =: \begin{bmatrix} M_{t,i} & 0 \\ * & M_{c,i}\end{bmatrix}, \quad M_{c,i} =: \begin{bmatrix} M_{k,k,i} & & \\ * & \ddots & \\ * & * & M_{k,1,i}\end{bmatrix} \text{ and } \quad N_i =: \begin{bmatrix}0\\ N_{c,i}\end{bmatrix}.$$

As for connection matrices in the univariate case, page 7, the entries of each $(k+1)^2\times(k+1)^2$ matrix M_i and each $(k+1)^2\times k(k+1)/2$ matrix N_i are derivatives of $\mathbf{r}_i$. $M_{t,i}$ corresponds to the $(k+2)(k+1)/2$ *homogeneous* constraints $\mathbf{j}^k\mathbf{p}_{i-1} = M_{t,i}\mathbf{j}^k\mathbf{p}_i$ that involve only derivatives of total degree k or less ($\bullet$ in Figures 8 and 9) and that can always be enforced by choosing one of the jets, say $\mathbf{j}^k\mathbf{p}_1$, and extending it to the remaining patches; that is, the total-degree k-jets represent a single polynomial expansion up to total degree k at the vertex, a characterization that is also known as the $n+1$-Tangent Theorem [78], [55].

Each submatrix $M_{c,i}$ corresponds to the remaining $k(k+1)/2$ constraints that involve derivatives of total degree greater than k (the diamonds $\diamond$ in Figure 8 and 9). By blockwise elimination, the rank of $\mathcal{M}$ equals $I-\prod M_i$ and the solvability for arbitrary right hand side depends, after removal of the homogeneous constraints, only on the rank of $I-\prod M_{c,i}$. Each submatrix $M_{c,i}$ decomposes further into skew upper triangular matrices $M_{k,\ell,i}$ of size $\ell\times\ell$ that are grouped along the diagonal.

Example For $k=1$ we have the constraints at 0 (c.f. Figure 9) and $\mathbf{r}_{ab} := D_1^aD_2^b\mathbf{r}\mid_0$

$$\begin{aligned}
00: &\quad D_1^0D_2^0\mathbf{p}_i = D_1^0D_2^0\mathbf{p}_{i+1}\\
01: &\quad D_1^0D_2^1\mathbf{p}_i = D_1^1D_2^0\mathbf{p}_{i+1}\\
10: &\quad D_1^1D_2^0\mathbf{p}_i = \lambda D_1^1D_2^0\mathbf{p}_{i+1} + \mu D_1^0D_2^1\mathbf{p}_{i+1}\\
11: &\quad D_1^1D_2^1\mathbf{p}_i = \mathbf{r}_{11}^{[1]}D_1^1D_2^0\mathbf{p}_{i+1} + \mathbf{r}_{11}^{[1]}D_1^0D_2^1\mathbf{p}_{i+1} + \lambda D_1^1D_2^1\mathbf{p}_{i+1} + \mu D_1^2D_2^0\mathbf{p}_{i+1}.
\end{aligned}$$

That is, dropping the subscript i for simplicity, each matrix-block $[MN]$ of G^1 constraints has the form

	00	10	01	11	20
00	1				
10		λ	μ		
01		1	0		
11		$\mathbf{r}_{11}^{[1]}$	$\mathbf{r}_{11}^{[2]}$	μ	λ

.

Here N is the last column, below '20'. The entries mn to the left of the matrix indicate that the row corresponds to the constraint $D_1^mD_2^n(\mathbf{p}_{i-1} - (\mathbf{p}_i\circ\mathbf{r}_i)) = 0$ while the entries on top indicate the derivatives $D_1^mD_2^n\mathbf{p}_i$ that enter the constraint as variables. For example, the column '20'

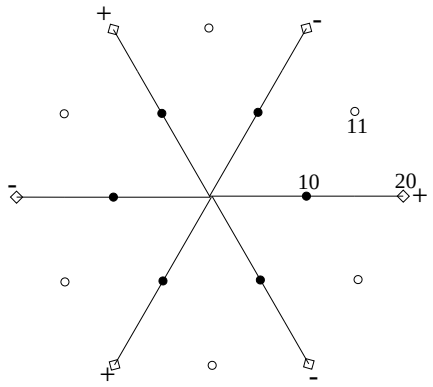

Figure 9. The total-degree 1-jet (•) represents the same linear function for all patches. The $\mathtt{n} = 6$ constraints involving the '11' derivatives $D_1^1 D_2^1$ (○) in the coordinate-degree 1-jet but not the total-degree 1-jet give rise to a 6×6 matrix M_c that is rank deficient by 1, i.e. of rank 5. This (vertex-enclosure) constraint can only be solved if the right hand side, defined by the (component normal to the tangent plane of the) '20' derivatives $D_1^2 D_2^0$ (◇), lies in the span of the constraint matrix. If all reparametrizations are the same, this is the case exactly when the alternating sum of the '20' derivatives is zero, i.e. if the average of the elements marked $+$ equals the average of the elements marked $-$.

corresponds to the variable $D_1^2 \mathbf{p}_i$. The constraint rows labeled '00','01', and '10' correspond to the total-degree 1-jet and are solvable leaving $\mathbf{j}^1\mathbf{p}_1$ free to determine the tangent plane by its three variables $D_1^0 D_2^0 \mathbf{p}_1 \mid_0 = \mathbf{p}_1(0)$, $D_1\mathbf{p}_1(0)$ and $D_2\mathbf{p}_1(0)$ with normal $\mathbf{n} = D_1\mathbf{p}_1(0) \wedge D_2\mathbf{p}_1(0)$. The (more interesting) constraint matrix M_c corresponds to the constraint row and column '11'. With $\mathbf{p}_i^{11} = \mathbf{n} \cdot D_1^1 D_2^1 \mathbf{p}_i$ and $\mathbf{p}_i^{20} = \mathbf{n} \cdot D_1^2 \mathbf{p}_i$

$$\begin{bmatrix} 1 & -\mu_1 & & \\ & 1 & -\mu_2 & \\ & & \ddots & \ddots \\ -\mu_{\mathtt{n}} & & & 1 \end{bmatrix} \begin{bmatrix} \mathbf{p}_1^{11} \\ \mathbf{p}_2^{11} \\ \vdots \\ \mathbf{p}_{\mathtt{n}}^{11} \end{bmatrix} = \begin{bmatrix} \lambda_1 \mathbf{p}_1^{20} \\ \lambda_2 \mathbf{p}_2^{20} \\ \vdots \\ \lambda_{\mathtt{n}} \mathbf{p}_{\mathtt{n}}^{20} \end{bmatrix}$$

By the Composition Constraint on page 12, $\prod_{i=1}^{\mathtt{n}} \mu_i = (-1)^{\mathtt{n}}$. Therefore the rank of the matrix is $\mathtt{n} - 1$ if $\mathtt{n}$ is even and $\mathtt{n}$ if $\mathtt{n}$ is odd [107], [108], [27], [124], [81], [28]. Moreover, if we assume symmetry, i.e. $\mu_i = -1$ and $\lambda_i = \lambda$ for $i = 1, \ldots, \mathtt{n}$, and if $\mathtt{n}$ is even then the vector $\mathbf{v}$ with $\mathbf{v}(i) = (-1)^i$ spans the null space of M_c and therefore the *Alternating Sum Constraint* has to hold for the system to be solvable (c.f. Figure 9): if $\lambda \neq 0$ then

$$0 = \sum_{i=1}^{\mathtt{n}} (-1)^i \mathbf{p}_i^{20}.$$

For $k = 2$, $[MN]$ has the form

	00	10	01	20	11	02	21	12	22	30	31	40
00	1											
10		λ	μ									
01		1	0									
20		$\mathbf{r}_{20}^{[1]}$	$\mathbf{r}_{20}^{[2]}$	λ^2	$2\lambda\mu$	μ^2						
11		$\mathbf{r}_{11}^{[1]}$	$\mathbf{r}_{11}^{[2]}$	λ	μ							
02				1								
21		$\mathbf{r}_{21}^{[1]}$	$\mathbf{r}_{21}^{[2]}$	A	B	C	$2\lambda\mu$	μ^2		λ^2		
12		$\mathbf{r}_{12}^{[1]}$	$\mathbf{r}_{12}^{[2]}$	D	E		μ			λ		
22		$\mathbf{r}_{22}^{[1]}$	$\mathbf{r}_{22}^{[2]}$	G	H	I	J	K	μ^2	L	$2\lambda\mu$	λ^2

where

$$A := \lambda D + \mathbf{r}_{20}^{[1]}, \quad B := \mu D + \lambda E + \mathbf{r}_{20}^{[2]}, \quad C := \mu E, D := 2\mathbf{r}_{11}^{[1]}, \quad E := 2\mathbf{r}_{11}^{[2]},$$

$$G := D^2/2 + 2\lambda\mathbf{r}_{12}^{[1]} + 2\mathbf{r}_{21}^{[1]}, \quad H := DE + 2\mu\mathbf{r}_{12}^{[1]} + 2\lambda\mathbf{r}_{12}^{[2]} + 2\mathbf{r}_{21}^{[2]}, \quad I := E^2/2 + 2\mu\mathbf{r}_{12}^{[2]},$$

$$J := 2\mu D + 2\lambda E, \quad K := 2\mu E, \quad L := 2\lambda D + \mathbf{r}_{20}^{[1]} + 2\lambda\mu.$$

For $k = 2$, $[MN]$ decomposes into the upper left 6×6 block M_t and, from columns '21', '12' and '22',

$$M_c = \begin{bmatrix} 2\lambda\mu & \mu^2 & \\ \mu & & \\ J & K & \mu^2 \end{bmatrix}, \quad M_{2,1} = \mu^2, \quad M_{2,2} = \begin{bmatrix} 2\lambda\mu & \mu^2 \\ \mu & \end{bmatrix}, \quad N_c = \begin{bmatrix} \lambda^2 & & \\ \lambda & & \\ L & 2\lambda\mu & \lambda^2 \end{bmatrix}.$$

◇

Remark: C, J and K above depend directly on D and E in the C^2 reparametrization matrix. To define a weaker notion of continuity in the spirit of Frénet-frame continuity for curves of Section 3.1 one would choose C, J and K independently.

For the remainder of the discussion we assume that all $\mathbf{r}_{ij}$ are linear and equal to $\mathbf{r}$, as in Lemma 2.1 (see [83] for a more general analysis and [29] and [122] for a discussion of the case $k = 2$ in terms of Bézier coefficients). Such equal reparametrization is the natural choice for filling '$\mathtt{n}$-sided holes' **??** and does not force symmetry of the patches: the tangent vectors, for example, need not span a regular $\mathtt{n}$-gon. If $\mathtt{n} = 4$ then $\operatorname{rank}(I - (M_{k,\ell})^{\mathtt{n}}) = 0$. That is, in the tensor-product case, since $N_c = 0$ one full coordinate-jet $\mathbf{J}^k\mathbf{p}_1$ can be chosen freely and $\mathbf{J}^k\mathbf{p}_2$, $\mathbf{J}^k\mathbf{p}_3$ and $\mathbf{J}^k\mathbf{p}_4$ are determined uniquely by the continuity constraints. For general $\mathtt{n}$, the rank deficiencies of $I - M_c^{\mathtt{n}}$ for $k = 1, 2, 3$ are listed in the following table. The results for larger k are sumarized in a conjecture in [83].

$\mathtt{n}$	k	1	2	3
3		0	2	2
4		1	3	6
6		1	2	4
even > 6		1	1	2
odd > 3		0	1	0

Since only the Taylor expansion is of interest, the vertex enclosure constraints are independent of the particular representation of the surrounding geometry maps. In particular, the vertex enclosure constraints apply to rational geometry maps in the same fashion as to polynomial geometry maps unless the denominator vanishes. The four known techniques for enforcing the vertex-enclosure constraints are listed in Section 4, page 24.

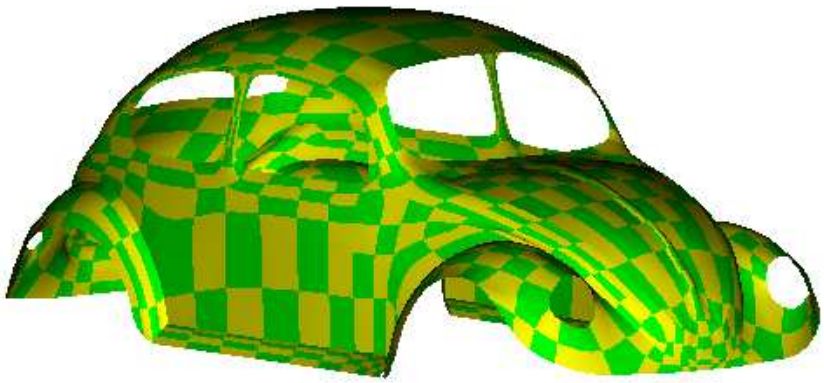

Figure 10. A free-form spline surface.

2.4. Free-form Surface Splines

One interpretation of the two types of maps defining the G^k free-form surface spline is that the reparametrizations $\mathbf{r}$ define an *abstract manifold* whose concrete *immersion* into $\mathbb{R}^3$ is defined by the geometry maps, e.g. Figure 10. Free-form surface splines have a bivariate control net with possibly n-sided facets and m-valent nodes. Alternative names are G-splines [61] and geometric continuous patch complexes [52]. Geometric continuous patch complexes differ in their characterization by requiring additionally a *connecting relation* that identifies (glues together) domain edges [52], [49], [100]. This connecting relation is needed when G^k continuity is defined in terms of the *existence* of reparametrizations rather than by explicitly identifying the (first $k+1$ Taylor terms of the) reparametrization.

Definition 2.6 *A G^k free-form surface spline is a collection of C^k geometry maps and at most one reparametrization $\mathbf{r}_{ij}$ for any pair of geometry maps $\mathbf{g}_i$, $\mathbf{g}_j$. The following constraints must hold.*

- *If the reparametrization $\mathbf{r}_{ij}$ exists then $\mathbf{g}_i$ and $\mathbf{g}_j$ join with geometric continuity G^k via $\mathbf{r}_{ij}$ along $\mathbf{g}_i(E)$, where E an edge of the domain Δ_i of $\mathbf{g}_i$, and $\mathbf{r}_{ij}$ is C^k.*
- *Any sequence of C^k geometry maps $\mathbf{g}_i : \Delta_i \mapsto \mathbb{R}^3, i = 1, \ldots, n$, such that $\mathbf{g}_i$ and $\mathbf{g}_{i+1}$ join G^k via $\mathbf{r}_{i,i+1}$ along $\mathbf{g}_{i+1}(E_{i+1})$, and $\mathbf{g}_i(E_i(0)) = Q$, meet G^k* with corner $Q \in \mathbb{R}^3$.

Free-form surface splines with different reparametrizations do not form a vector space. This follows directly from the same statement for G^k continuous curves. For example, we can replace lines with planes in the example shown in Figure 5. However, if all reparametrizations agree then we can form average free-form surface splines and the average inherits the continuity by linearity of differentiation. Section 4 outlines constructions.

3. Equivalent and Alternative Definitions

3.1. Matching Intrinsic Curve Properties

In [13], Boehm argues that there are (only) two types of geometric continuity: contact of order k, a notion equivalent to G^k continuity, and, secondly, continuity of geometric invariants

(but not necessarily of their derivatives).

Two abutting curve segments have *contact of order* k if they are each the limit of a sequence of curves that intersect in $k+1$ points, as these points coalesce. In particular, for a space curve $\mathbf{x} : \mathbb{R} \mapsto \mathbb{R}^3$ with Frénet frame **??** spanned by the tangent vector $\mathbf{t}$, the normal vector $\mathbf{m}$ and the binormal $\mathbf{b}$ and $'$ denoting the derivative with respect to *arc length*

$$\begin{aligned} \mathbf{x}'' = \mathbf{t}' &= \kappa \mathbf{m}, & \kappa &= \text{vol}_2[\mathbf{x}', \mathbf{x}''], \\ \mathbf{x}''' = \mathbf{t}'' &= -\kappa^2 \mathbf{t} + \kappa' \mathbf{m} + \kappa\tau \mathbf{b} & \tau\kappa^2 &= \text{vol}_3[\mathbf{x}', \mathbf{x}'', \mathbf{x}'''], \end{aligned}$$

contact of order 2 implies that $\mathbf{x}' = \mathbf{t}$ and $\mathbf{x}''$ are continuous and therefore that tangent, normal and curvature are continuous. Contact of order 3 implies continuity of $\mathbf{x}'$, $\mathbf{x}''$ and $\mathbf{x}'''$ and therefore continuity of Frénet frame, curvature and torsion. Moreover, the *derivative of the curvature must be continuous* tying the entry labeled α in the connection matrix displayed on page 7 in Section 2.1 to quantities already listed in the matrix. Similarly, contact of order k in $\mathbb{R}^3$ requires $\kappa \in C^{k-2}$ and $\tau \in C^{k-3}$ and therefore further dependencies among the entries [41].

By contrast, continuity of the kth geometric invariant, also called *kth order Frénet frame continuity* [30], [37], and abbreviated F^k, does not require that the α-entry (or, more generally, any subdiagonal entry) depend on other entries in the connection matrix. Frénet frame continuity requires that the frame of the two curve pieces agrees and only makes sense in $\mathbb{R}^d$, for $d \geq k$. Boehm [13] shows that while geometric continuity is projectively invariant, Frénet frame continuity is not. For surfaces, an analogous notion of continuity in terms of fewer restrictions on the connection matrix entries, is pointed out on page 16.

3.2. C^k Manifolds

Differential geometry has a well-established notion of continuity for a point set: to verify kth order continuity, we must find, for every point Q in the point set, an invertible C^k map (chart) that maps an open surface-neighborhood of Q into an open set in $\mathbb{R}^2$. If two surface-neighborhoods, with charts $\mathbf{q}_1$ and $\mathbf{q}_2$ respectively, overlap then $\mathbf{q}_2 \circ \mathbf{q}_1^{-1} : \mathbb{R}^2 \mapsto \mathbb{R}^2$ must be a C^k function. This notion of continuity is not constructive: while it defines when a point set can be given the structure of a C^k manifold, say a C^k surface, it neither provides tools to build a C^k surface nor a mechanism suitable for verification by computer.

However, geometric continuity and the continuity of manifolds are closely related: every point in the union of the patches of a G^k free-form surface spline admits local parametrization by C^k charts if the surface does not self-intersect: the union is an immersed C^k surface with piecewise C^k boundary. We face two types of obstacles in establishing this fact. First, the geometry maps should not have geometric singularities on their respective domains since these would prevent invertibility of the charts, and the spline should not self-intersect so that we can map a neighborhood of the point in $\mathbb{R}^3$ to the plane in a 1-1 fashion. Establishing regularity and non-self-intersection requires potentially expensive intersection testing **??**. The second apparent obstacle is that the patches that make up the surface are *closed sets that join without overlap*. Therefore the geometry maps cannot directly be used as charts. However, as illustrated in Figure 11, we can think of the charts as piecewise maps composed of $\mathtt{n}$ maps $\mathbf{q}_i = \mathbf{r}_i^{-1} \circ \mathbf{g}_i^{-1}$ that map open neighborhoods in $\mathbb{R}^3$ (grey oval) to open neighborhoods in $\mathbb{R}^2$ (grey disk).

3.3. Tangent and Normal Continuity

A number of alternative characterizations exist to test a given G^1 free-form spline complex for tangent continuity or derive G^1 free-form splines. The criteria consist of an equality constraint

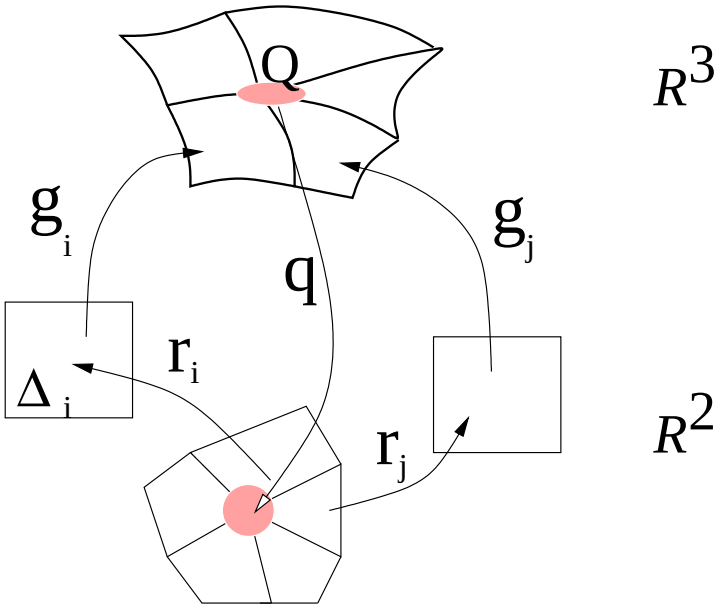

Figure 11. In the neighborhood of Q a free-form surface spline with reparametrizations $\mathbf{r} = \mathbf{r}_i \circ \mathbf{r}_j^{-1}$ can be viewed as a manifold with chart consisting of pieces $\mathbf{q}_i = \mathbf{r}_i^{-1} \circ \mathbf{g}_i^{-1}$, $i = 1, \ldots, \mathtt{n}$.

establishing coplanarity of the first partial derivatives at each point of the common boundary of two patches (c.f. Figure 4), and an inequality constraint on the reparametrization that prevents a $180°$-flip of the normal for the regular geometry maps. In the following lemma, e is the direction along the preimage E of the common boundary $\mathbf{p}(E)$ and, as is appropriate for least degree polynomial representations (see 9), $\mathbf{p}$ and $\mathbf{g}$ share have the same parametrization along $\mathbf{p}(E)$

Lemma 3.1 (Tangent continuity) *Let* $\mathbf{p}$ *and* $\mathbf{g}$ *be regular parametrizations and* $\mathbf{p} \mid_E = \mathbf{g} \mid_E$. *The maps* λ, μ *and* ν *are univariate scalar-valued function and*

$$\begin{aligned}
\mathbf{c} &:= D_e\mathbf{p} \mid_E = D_e\mathbf{g} \mid_E, \\
\mathbf{n} &:= \mathbf{c} \wedge D_{e^\perp}\mathbf{g} \mid_E \\
\bar{\mathbf{n}} &:= -\mathbf{c} \wedge D_{e^\perp}\mathbf{p} \mid_E, \\
\mathbf{t} &:= \mathbf{n} \wedge \mathbf{c}
\end{aligned}$$

are vector-valued functions maping to $\mathbb{R}^3$ *parametrized over the edge* E. *Then the following characterizations of* G^1 *continuity are equivalent.*

$$\begin{aligned}
&(1e) \quad D_{e^\perp}\mathbf{p} = \alpha_{\mathbf{p}}\mathbf{t} + \beta_{\mathbf{p}}\mathbf{c},\ D_{e^\perp}\mathbf{g} = \alpha_{\mathbf{g}}\mathbf{t} + \beta_{\mathbf{g}}\mathbf{c} && \alpha_{\mathbf{p}}\alpha_{\mathbf{g}} < 0, && (1i) \\
&(2e) \quad \lambda\mathbf{c} = \mu D_{e^\perp}\mathbf{g} \mid_E + \nu D_{e^\perp}\mathbf{p} \mid_E, && \mu\nu > 0, && (2i) \\
&(3e) \quad \det\left[\mathbf{c}, D_{e^\perp}\mathbf{g} \mid_E, D_{e^\perp}\mathbf{p} \mid_E\right] = \mathbf{n} \cdot D_{e^\perp}\mathbf{p} \mid_E = 0, && \mathbf{n} \cdot \bar{\mathbf{n}} > 0, && (3i) \\
&(4e) \quad \frac{\bar{\mathbf{n}}}{\|\bar{\mathbf{n}}\|} = \frac{\mathbf{n}}{\|\mathbf{n}\|},
\end{aligned}$$

With $D\mathbf{r}\mid_E = [\frac{\lambda}{\nu}\frac{\mu}{\nu}]$, (2) is the definition of a G^1 join in Definition 2.3. Figure 4 illustrates the geometric meaning of (2). *Proof* Regularity implies $\mathbf{n}(t) \neq 0$ for all t on E.
(1) $\implies$ (2): Adding the two equalities (1e) after multiplication with $\nu = -\alpha_{\mathbf{g}}$ and $\mu = \alpha_{\mathbf{p}}$ respectively (2e) holds in the form $\alpha_{\mathbf{p}} D_{e^\perp}\mathbf{g} - \alpha_{\mathbf{g}} D_{e^\perp}\mathbf{p} = (\alpha_{\mathbf{p}}\beta_{\mathbf{g}} - \alpha_{\mathbf{g}}\beta_{\mathbf{p}})\mathbf{c}$.
(2) $\implies$ (3): The inner product of both sides of (2e) with $\mathbf{n}$ yields (3e). The cross product $\wedge$ of (2e) with $\mathbf{c}$ followed by the inner product $\cdot$ with $\mu\mathbf{n}$ yields $0 = \mu^2\|\mathbf{n}\|^2 - \mu\nu\mathbf{n}\cdot\bar{\mathbf{n}}$. Then (2i) implies (3i).
(3) $\implies$ (4): From (3e) we have $\mathbf{n} \perp D_{e^\perp}\mathbf{p}$ and, by definition, $\mathbf{n} \perp \mathbf{c}$. By regularity $\mathbf{n}/\|\mathbf{n}\| = \pm\bar{\mathbf{n}}/\|\bar{\mathbf{n}}\|$ and (3i) decides the sign.
(4) $\implies$ (1): Regularity and (4) imply (1e) that the partial derivatives $D_{e^\perp}\mathbf{p}$ and $D_{e^\perp}\mathbf{g}$ can be expressed in the same (orthogonal) coordinate system spanned by $\mathbf{t}$ and $\mathbf{c}$. The cross product of each equality with $\mathbf{c}$ yields $-\bar{\mathbf{n}} = \alpha_{\mathbf{p}}\mathbf{c}\wedge\mathbf{t}$ and $\mathbf{n} = \alpha_{\mathbf{g}}\mathbf{c}\wedge\mathbf{t}$ and by sign comparison (1i). $\bowtie$

Formulation (4), comparison of normals, can be turned into a practical tool for quantifying tangent discontinuity. While (1), (2) and (3) are unique only up to scaling, and therefore 'ϵ-discontinuity' measured as $\epsilon > \|\alpha_{\mathbf{p}}\mathbf{t} + \beta_{\mathbf{p}}\mathbf{c} - D_{e^\perp}\mathbf{p}\|$ or $\epsilon > \|\mu D_{e^\perp}\mathbf{g} + \nu D_{e^\perp}\mathbf{p}, -\lambda D_e\mathbf{g}\|$ or $\epsilon > |\mathbf{n}\cdot D_{e^\perp}\mathbf{p}|$ is not well-defined, the *angle* between the two normals is scale-invariant.

The symmetric characterization (1) asserts the existence of a Taylor expansion along the boundary that is matched by $\mathbf{g}$ and $\mathbf{p}$ It has been used for constructions [16], [80], [101]. The direct equivalence of (1) and (2) for polynomials is proven in [22] and [54] generalizes this Taylor-expansion approach to kth order.

If $\mathbf{p}$ and $\mathbf{g}$ are *rational* maps, i.e. quotients of polynomials, the continuity conditions can be discussed in terms of polynomials in *homogenous coordinates* keeping in mind that we may scale freely by a scalar-valued function $\sigma(u,v)$: $D^\kappa\mathbf{p}\mid_E = D^\kappa(\sigma\mathbf{g}\circ\mathbf{r})\mid_E, \quad \kappa = 0,\ldots,k$ [123].

If $\mathbf{p}$ and $\mathbf{g}$ are *polynomials* then, up to a common factor, so are the scalar functions, λ, μ and ν in (1). In fact, after removal of common factors, the degree of the functions is bounded by the degree of $\mathbf{p}$ and $\mathbf{g}$. This comes in handy when looking for possible reparametrizations $\mathbf{r}$ between two geometry maps.

Lemma 3.2 *If* $\mathbf{p}$ *and* $\mathbf{g}$ *are polynomials, then, up to a common factor,* λ, μ *and* ν *in (1) are polynomials of degree no larger than respectively*

$$\textit{degree}(D_{e^\perp}\mathbf{g}) + \textit{degree}(D_{e^\perp}\mathbf{p}), \quad \textit{degree}(D_e\mathbf{g}) + \textit{degree}(D_{e^\perp}\mathbf{p}) \textit{ and}$$
$$\textit{degree}(D_e\mathbf{g}) + \textit{degree}(D_{e^\perp}\mathbf{g}).$$

Proof Due to regularity of $\mathbf{g}$ along the boundary, the pre-image of the boundary is covered by overlapping intervals U such that for each U there are two components $i,j \in \{x,y,z\}$ with $\det M_{ij} \neq 0$, $M_{ij} := \begin{bmatrix} D_e\mathbf{g}^{[i]} & D_{e^\perp}\mathbf{g}^{[i]} \\ D_e\mathbf{g}^{[j]} & D_{e^\perp}\mathbf{g}^{[j]} \end{bmatrix}$, $\mathbf{g}^{[j]}$ the jth component of $\mathbf{g}$. Therefore we can apply Cramer's rule to

$$M_{ij}\begin{bmatrix}\lambda\\ -\mu\end{bmatrix} = \nu\begin{bmatrix} D_{e^\perp}\mathbf{p}^{[i]} \\ D_{e^\perp}\mathbf{p}^{[j]}\end{bmatrix}$$

and obtain

$$\begin{bmatrix}\lambda\\ -\mu\\ \nu\end{bmatrix} = \frac{\nu}{\det M_{ij}}\begin{bmatrix} -\det\begin{bmatrix} D_{e^\perp}\mathbf{p}^{[i]} & D_{e^\perp}\mathbf{g}^{[i]} \\ D_{e^\perp}\mathbf{p}^{[j]} & D_{e^\perp}\mathbf{g}^{[j]}\end{bmatrix} \\ \det\begin{bmatrix} D_e\mathbf{g}^{[i]} & D_{e^\perp}\mathbf{p}^{[i]} \\ D_e\mathbf{g}^{[j]} & D_{e^\perp}\mathbf{p}^{[j]}\end{bmatrix} \\ \det\begin{bmatrix} D_{e^\perp}\mathbf{g}^{[i]} & D_e\mathbf{g}^{[i]} \\ D_{e^\perp}\mathbf{g}^{[j]} & D_e\mathbf{g}^{[j]}\end{bmatrix}\end{bmatrix}.$$

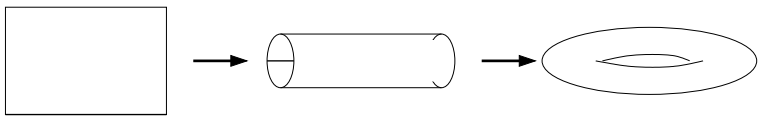

Figure 12. A global periodic parametrization.

The degree of λ, μ and ν is bounded by the degrees of the determinants since the common factor $\nu/\det M_{ij}$ can be eliminated in the constraints. Since $\det M_{ij}$ vanishes at most at isolated points the degree bound extends from U to the whole interval. ⋈

The characterizations of geometric continuity in terms of geometric invariants (tangents, curvatures) are characterizations of continuity by covariant derivatives [52].

Lemma 3.3 *Two C^k geometry maps* $\mathbf{p}$ *and* $\mathbf{g}$ join with geometric continuity G^k *via the C^k reparametrization* $\mathbf{r}$ *along* $\mathbf{p}(E)$ *if there exist normal vector fields* $\mathbf{n_p}$ *and* $\mathbf{n_g}$ *of* $\mathbf{p}$ *and* $\mathbf{g}$ *respectively such that*

$$D^\kappa \mathbf{n_p} \mid_E = D^\kappa \mathbf{n_g} \mid_{\mathbf{r}(E)}, \kappa = 0, \ldots, k-1.$$

In particular, $D\mathbf{n}$ represents the shape operator [67], principal curvatures and directions [116], [57] or the Dupin indicatrix [66]. [57] shows in particular equivalence of G^2 continuity with curvature continuity based on sharing surface normal, principal curvatures and principle curvature directions in $\mathbb{R}^3$.

3.4. Global and Regional Reparametrization

Often we can view a free-form surface as a *function* over a domain with the same topological genus, e.g. an isosurface of the electric field surronding the earth may be computed as a function over a sphere [1]. More generally, we can assemble an object of the appropriate topological genus by identifying edges of a planar domain and then define a standard spline space over the planar domain, mapping into $\mathbb{R}^3$ with additional periodic boundary conditions and creating 'orbifolds' [34], [119]. This approach circumvents the need for relating many individual domains via reparametrizations, since there is only one *global* domain (modulo periodicity). Basis functions with local support in the domain yield local control. For practical use one has to consider three points. First, the genus of the object has to be fixed before the detailed design process can begin – so one cannot smoothly attach an additional handle later on. Second, the spline functions have to be placed with a density that anticipates for example, an ornate protrusion of the surface where more detail control is required. Third, the 'hairy ball theorem': you cannot smoothly comb the hair of a hairy ball without leaving a bald spot or making a parting, implies that the global mapping from subsets of the plane to, say, the sphere has a singularity. The theorem, a consequence of the Borsuk-Ulam theorem, states more formally "If $f : S^2 \mapsto S^2$ is a continuous map from the sphere to itself then there exists a point where x and $f(x)$ are not orthogonal as vectors in $\mathbb{R}^3$" and in particular, with x a point on the sphere S^2 and $f(x)$ a corresponding unit tangent, "the tangent field on a sphere in $\mathbb{R}^3$ has to have a singularity". The singularity is nicely illustrated in [56].

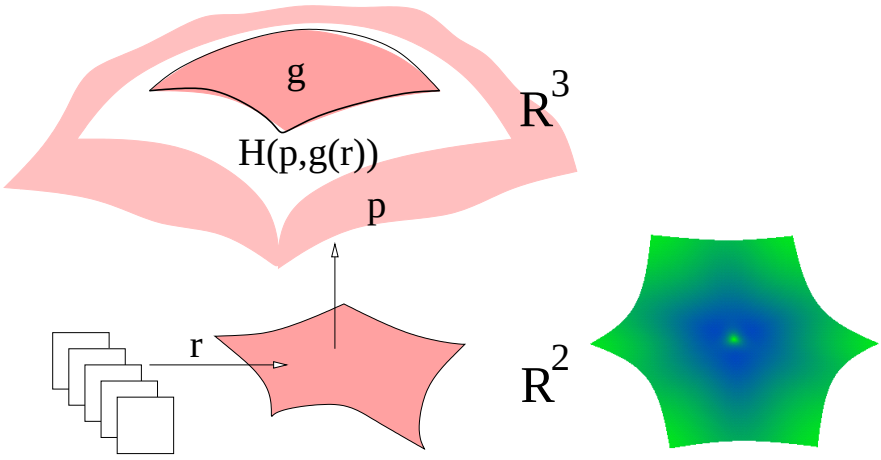

Figure 13. (*left*) Regional parametrization: an n-sided cap $\mathbf{g}$ is Hermite-extended via $H(\mathbf{p}, \mathbf{g}\circ\mathbf{r})$ to match a given spline complex $\mathbf{p}$. (*right:*) Gauss curvature at a higher-order saddle point: the central point must have zero curvature.

Prautzsch [95], and co-workers [75],[96], and Reif [98], [100] developed the idea of filling n-sided holes by building a *regional parametrization* $\mathbf{r}$ for a neighborhood of a point Q where n patches meet (see Figure 13). The regional parametrization stands in contrast to the local reparametrizations along an edge used to define free-form surface splines, and the global parametrization discussed earlier. The regional parametrization is composed with a single map $\mathbf{g}$, for example a quadratic polynomial. This approach considerably simplifies reasoning about the resulting surfaces. By separating issues of geometric shape from valence and local topology, verification of smoothness of the resulting surfaces at Q (which could be a major effort of symbolic computing) reduces to showing that $\mathbf{r}$ is smooth since smoothness is preserved under composition with an (infinitely smooth) polynomial geometry map. Reparametrization gives $\mathbf{g} \circ \mathbf{r}$ the structure of a collection of standard (tensor-product or total-degree) patches that can then be connected to a surrounding ring of spline patches $\mathbf{p}$ via Hermite interpolation $H(\mathbf{p}, \mathbf{g}\circ\mathbf{r})$ of degree (degree of $\mathbf{g}$ times degree of $\mathbf{r}$). By fixing the degree d of the polynomial beforehand, independent of the smoothness k to be achieved, and choosing the C^k parametrization in the domain to be of bidegree $(k+1)$, the regional schemes were the first to claim a construction of C^k surfaces of a degree linear in k, namely of degree $d(k+1)$. In particular, Prautzsch and Reif proposed to choose polynomials of degree $d = 2$ which yields G^2 free-form constructions of degree bi-6.

Fixing the degree of $\mathbf{g}$ comes at a cost. While quadratics come in a large number of shapes [89] they are not able to model, for example, higher-order saddle points. A *higher-order saddle point* is a point on a C^2 surface with three or more extremal curvature directions; hence it has zero curvature as illustrated in Figure 13, *right*. However, quadratics that have a point of zero curvature must be linear and this yields flat patches rather than a flat point. For the particular example of a 3-fold saddle point, we could address this shortcoming by increasing the degree of the polynomial to three and the overall degree to bi-9 [100]. But this does not address the

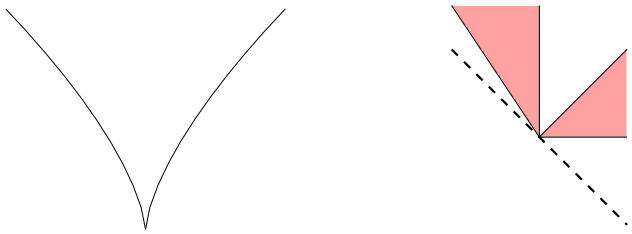

Figure 14. (*left*) Zero set of $x^2 + y^3 = 0$ and (*right*) tangent sectors of two possibly smooth patches whose relative position does not allow the reduction to smoothness of a curve by cutting with a transversal plane (dashed line).

underlying problem, namely the mismatch between $\mathtt{n}$ patches meeting at Q and the fixed number of coefficients of any single polynomial of fixed degree d. In [86] it was therefore suggested to replace $\mathtt{g}$ by a (total-degree cubic) spline. This yields at least $\mathtt{n}$ degrees of freedom.

3.5. Implicit Representation

Under suitable monotonicity and regularity constraints the zero set of a trivariate polynomials in BB-form over a unit simplex defines a *single-sheeted, singly connected* piece of surface that we can also call a patch **??**. If $p, q : \mathbb{R}^3 \mapsto \mathbb{R}$ are two trivariate polynomials in BB-form that join C^k as functions at a common point $E \in \mathbb{R}^3$ or across a common curve $E \in \mathbb{R}^3$ then generically (see caveat below) the corresponding patches join with *contact of order k at E*: E is the limit of $k+1$ intersection points (curves) E_j of functions p_j and q_j converging respectively $E_j \mapsto E$, $p_j \mapsto p$ and $q_j \mapsto q$. Just as in the parametric case, we have to make sure that the trivariate polynomials are regular at E, as the following example demonstrates: Let $p(x, y, z) = x^2 + y^3, x \leq 0$, $q(x, y, z) = x^2 + y^3, x \geq 0$. Both p and q are polynomial pieces, have single-sheeted, singly connected zero sets and join C^k for any k; but the zero set is not smooth at the intersection (see Figure 14 *left* for a cross-section.)

Since we are only concerned with the zero set of the polynomial we do not actually need that the polynomials join smoothly but can scale the joining pieces by scalar functions a and b ([121], [120], [71]):

Definition 3.1 *Two trivariate polynomials p and q join with G^k continuity at Q if*

$$\mathbf{j}^k(p \cdot a) \mid_Q = \mathbf{j}^k(q \cdot b) \mid_Q, \quad a(Q) \neq 0, b(Q) \neq 0.$$

Two trivariate polynomials p and q join with G^k continuity at an irreducible curve $E = (q = 0) \cap (h = 0)$ if

$$\mathbf{j}^k p = \mathbf{j}^k(aq + bh^{k+1}), \quad a(E) \neq 0, b(E) \neq 0.$$

One could intersect E with a transversal plane to avoid a separate definition for continuity along E by reducing it to the point intersection. (The analogous technique for parametric surfaces is called Linkage Curve Theorem [78], [55].) This approach, however, runs into technical problems, since implicit *patches* have corners and there may be just one point of intersection

with a transversal plane. Similarly, the trivariate k-jet $\mathbf{j}^k p$ cannot just be replaced by a k-jet along a line [35] since the domains may lie in the same half space and thus there is no plane that intersects both *restricted* domains in more than the common point (see Figure 14, *right*.)

3.6. Generalized Subdivision

Near $\mathtt{n}$-valent mesh nodes, uniform generalized subdivision surfaces consist of an infinite sequence of ever smaller, concentric rings that are internally parametrically C^k. The rings also join one another parametrically C^k. Yet, by the Borsuk-Ulam theorem (Section 3.4) there cannot be a parametrically C^k mapping from the plane to objects of arbitrary genus without a singularity. In a sense the (effect of the) necessary reparametrization is therefore concentrated in the $\mathtt{n}$-valent mesh nodes. Correspondingly the analysis of smoothness of generalized subdivision surfaces has therefore focused on the limits of the $\mathtt{n}$-valent mesh nodes (see e.g. [3] [90], [91]). At present it appears that uniform generalized subdivision cannot generate curvature continuous surfaces unless the control net is in special position.

4. Constructions

An algorithm for constructing C^k surfaces subject to data, such as a control net or a prescribed network of curves, is a specification of the C^k reparametrizations $\mathbf{r}$ up to kth order and of the geometry maps $\mathbf{g}$ (see also $\mathtt{n}$-sided hole filling **??**).

The *generic approach* of stitching together individual spline patches consists of

- choosing a consistent reparametrization $\mathbf{r}$ at the $\mathtt{n}$-valent points and deriving a reparametrization for two edge-ajacent patches as a Hermite interpolant to the reparametrizations at the end points of the edge; and

- solving the vertex-enclosure problem at each point and deriving the geometry maps of abbutting patches as a Hermite interpolant to the Taylor expansions at the vertices.

The *generic construction* is as follows.
(1) If $\mathtt{n}_0$ patches join at one boundary endpoint, corresponding to $s = 0, t = 0$, and $\mathtt{n}_1$ patches join the other with $s = 1, t = 0$ then a Hermite interpolant (in s) to the linear symmetric reparametrization of Lemma 2.1 at the endpoints, up to kth order is given by

$$\mathbf{r}(t, s) = (s + 2th(s),\ -t), \qquad h(s) = \alpha(s) \cos \frac{2\pi}{\mathtt{n}_0} - \beta(s) \cos \frac{2\pi}{\mathtt{n}_1},$$

where $\alpha(s)$ and $\beta(s)$ are C^k functions such that $\alpha(s), \beta(s) \geq 0$,

$$\alpha(0) = \beta(1) = 1, \alpha(1) = \beta(0) = 0, \quad D^\kappa \alpha(i) = D^\kappa \beta(i) = 0, i \in \{0, 1\}, \kappa > 1.$$

The interpolant is minimal in that the Taylor expansions of the reparametrization at either endpoint do not interfere, i.e. $D_2^\kappa \mathbf{r}(i) = 0$ for $i \in \{0, 1\}$, $\kappa > 1$ [46].
(2) The vertex-enclosure problem (for example for G^1, $\mathtt{n}$ even) can be solved by one the following four techniques [81]:

1. Choosing H_i^k (e.g. the curve mesh) in the span of the constraint matrix $\mathcal{M}$;

2. Splitting patches whose boundaries are prescribed into two or more pieces so that the boundary curves of the split patches can be freely chosen in the span of the constraint matrix (e.g. [31], [32], [92]);

3. Using rational patches to introduce second-order poles at the vertices (e.g. [42], [16] [53]);

4. Using a non-regular parametrization [81], [76], [98].

Thus, if we are not concerned about the degree, it is straightforward to create G^k free-form surface splines for any k. The focus over the past decade has been to reduce the degree of the surface representation, and to obtain better surface shapes **??**. For example, while the degree of curvature continuous surfaces prior to [95] and [98] was at least bi-9 (100 coefficients per patch) [127], [51] newest results achieve curvature continuity with at most 24 coefficients per patch [87].

Some special the techniques (c.f. Lemma 3.1) are as follows.

- Given the common boundary with derivative $\mathbf{c} = D_e\mathbf{p} \mid_E = D_e\mathbf{g} \mid_E$, [16], [80], [22] use a *symmetric* construction, picking $\mathbf{t}$ as minimal Hermite interpolant to the transversal derivative data at the endpoints and

$$D_{e^\perp}\mathbf{p} = \alpha_{\mathbf{p}}\mathbf{t} + \beta_{\mathbf{p}}\mathbf{c}, \qquad D_{e^\perp}\mathbf{g} = \alpha_{\mathbf{g}}\mathbf{t} + \beta_{\mathbf{g}}\mathbf{c}$$

  with $\mathbf{t} \wedge \mathbf{c} \neq 0$ and $\alpha_{\mathbf{p}} \neq 0 \neq \alpha_{\mathbf{g}}$.

- As illustrated in Figure 5 the average of two G^1 joined curves or surfaces is generally not G^1. But if all transversal derivatives of a patch along a boundary $E(t)$ are *collinear* with a vector $\mathbf{v}$, i.e.

$$D_{e^\perp}\mathbf{p} \mid_E = p(t)\mathbf{v} \text{ and } D_{e^\perp}\mathbf{q} \mid_E = q(t)\mathbf{v}$$

  for scalar functions p and q with $q/p < 0$ then $\mathbf{n} = N/\|N\|$ where $N(t) := D_e\mathbf{p} \mid_E \wedge \mathbf{v}$ is a normal common to both patches along the boundary [99].

- Sabin [105] and [79] use formulation (2) of Lemma 3.1, $\mathbf{n} \wedge D\mathbf{p} = 0$, to determine versal and transversal derivatives of $\mathbf{p}$ – thereby *isolating* the construction of a patch from its neighbor.

- [72] and [80] list a number of choices for reparametrizations for particular constructions.

4.1. Free-form Surface Splines of Low Degree

Goodman [36] introduced G^1 splines of degree *bi-2* for special control meshes that consist of quadrilateral facets and vertices of valence 3 or 4. The prototype meshes, that can be modified by quadrilateral refinement, the cube mesh and the dual of the cube with lopped off corners, are sphere-like shapes that, when symmetric, are curvature continuous (see [88]). Splitting each original quadrilateral facet 1-4, [99] derives a bi-2 G^1 free-form surface spline. Splitting each quadrilateral facet into four triangles, [85] obtains a G^1 construction of total degree 3 that also satisfies the local convex hull property, i.e. the surface points are guaranteed to be an average of the local control mesh. All constructions with quadratic boundary curve, however, suffer from

a shape defect when they are to model a higher-order saddle point : due to the Alternating Sum Constraint on page 2.3.2 the quadratic boundary curves must lie on a straight line.

The G^k free-form spline constructions of Prautzsch [95] and Reif [98] are of degree $2(k+1)$ if flat regions at higher-order saddle points are acceptable – and of degree $r(k+1)$ if modeling of the local geometry requires a polynomial of degree r. [48] shows that a degree bi-5 construction should be possible and [87] models curvature continuous free-form surfaces of unrestricted patch layout from patches of maximal degree $d + 2 \times 3$, $d > 0$ with the flexibility of degree d, C^2 splines at extraordinary points.

5. Additional Literature

Every paper on smooth surfacing defines some, possibly specialized, notion of geometric continuity. Some of the early characterizations can be found in [10] [9],[8] [23] [27] [31] [33] [69] [72] [74] [77] [104,103] [106], [107], [108], [114], [112], [113], [45], , [82], [92], [117], [115] [116] [126] [116] [125] and characterizations for curves in [6], [7], [50],[20], [30].

A number of publications specifically aim at clarifying the notion of geometric continuity. Kahmann discusses curvature and the chain rule [66], DeRose [23] reconciles continuity after reparametrization with the smoothness of manifolds (see also [25], [26]). Liu [73]characterizes C^1 constraints in the form (1) of Lemma 3.1. Particularly well-illustrated is Boehm's treatment of geometric and 'visual' continuity [11], [12] [14], [13]. Herron [57] shows directly the equivalence of first and second order geometric continuity with tangent and curvature continuity of surfaces. Further characterizations can be found in [62], [94,93],[22], [54], [24], [122], [118].

Hahn's treatment of geometric continuity [52] (see also [41]) served as a blueprint for Section 2 but differs in that he defines a G^k join in terms of the existence of a reparametrization, rather than making the reparametrization part of the definition.

Warren's thesis [121] looks at geometric continuity of implicit representations and [35] is a tour de force of conversions of notions of geometric continuity between two patches.

I am indebted to *Tamas Hermann* for closely reading the article and making numerous suggestions.

REFERENCES

1. Peter Alfeld, Marian Neamtu, and Larry L. Schumaker. Bernstein-Bézier polynomials on spheres and sphere-like surfaces. *Computer Aided Geometric Design*, 13(4):333–349, 1996.
2. Peter Alfeld and Larry L. Schumaker. On the dimension of bivariate spline spaces of smoothness r and degree $d = 3r + 1$. *Numerische Mathematik*, 57(6/7):651–661, July 1990.
3. A.A. Ball and D.J.T. Storry. Conditions for tangent plane continuity over recursiveley generated b-spline surfaces. *ACM Transactions on Graphics*, 7(2):83–102, 1988.
4. R. Barnhill and J. Gregory. Compatible smooth interpolation in triangles. *J of Approx. Theory*, 15(3):214–225, 1975.
5. Phillip J. Barry, Nira Dyn, Ronald N. Goldman, and Charles A. Micchelli. Identities for piecewise polynomial spaces determined by connection matrices. *Aequationes Math.*, 42(2-3):123–136, 1991.

6. Brian A. Barsky. *The Beta-spline: A Local Representation Based on Shape Parameters and Fundamental Geometric Measures*. Ph.d. thesis, University of Utah, December 1981.
7. Brian A. Barsky and Tony D. DeRose. Geometric continuity of parametric curves: Three equivalent characterizations. *IEEE Computer Graphics and Applications*, 9(6):60–69, November 1989.
8. E. Beeker. Smoothing of shapes designed with free-form surfaces. *Computer-Aided Design*, 18(4):224–232, May 1986.
9. P. Bézier. *Numerical Control: Mathematics and Applications*. Wiley, 1972. translated by R. Forrest.
10. Pierre E. Bezier. *Essai de definition numerique des courbes et des surfaces experimentales*. Ph.d. thesis, Universite Pierre et Marie Curie, February 1977.
11. W. Boehm. Curvature continuous curves and surfaces. *Computer-Aided Design*, 18(2):105–106, March 1986.
12. W. Boehm. Smooth curves and surfaces. In G. Farin, editor, *Geometric Modeling: Algorithms and New Trends*, pages 175–184. SIAM, Philadelphia, 1987.
13. Wolfgang Boehm. On the definition of geometric continuity. *Computer-Aided Design*, 20(7):370–372, 1988. Letter to the Editor.
14. Wolfgang Boehm. Visual continuity. *Computer-Aided Design*, 20(6):307–311, 1988.
15. H. Bohl and U. Reif. Degenerate Bézier patches with continuous curvature. *Comput. Aided Geom. Design*, 14(8):749–761, 1997.
16. H. Chiyokura and F. Kimura. Design of solids with free-form surfaces. In *Computer Graphics (SIGGRAPH '83 Proceedings)*, volume 17(3), pages 289–298, July 1983.
17. G. M. Constantine and T. H. Savits. A multivariate Faà di Bruno formula with applications. *Trans. Amer. Math. Soc.*, 348(2):503–520, 1996.
18. S. A. Coons. SURFACES FOR COMPUTER-AIDED DESIGN OF SPACE FORMS. Technical Report MIT/LCS/TR-41, Massachusetts Institute of Technology, June 1967.
19. Carl de Boor, Klaus Höllig, and Malcolm Sabin. High accuracy geometric hermite interpolation. *Computer Aided Geometric Design*, 4(4):269–278, December 1987.
20. W. L. F. Degen. Some remarks on bézier curves. *Computer Aided Geometric Design*, 5(3):259–268, August 1988.
21. W. L. F. Degen. High accurate rational approximation of parametric curves. *Computer Aided Geometric Design*, 10(3):293–314, August 1993.
22. Wendelin L. F. Degen. Explicit continuity conditions for adjacent Bézier surface patches. *Computer Aided Geometric Design*, 7(1-4):181–189, June 1990.
23. T. DeRose. *Geometric Continuity: A Parametrization Independent Measure of Continuity for Computer Aided Design*. PhD thesis, UC Berkeley, California, 1985.
24. T. D. DeRose. Necessary and sufficient conditions for tangent plane continuity of Bézier surfaces. *Computer Aided Geometric Design*, 7(1–4):165–179, June 1990.
25. T. D. Derose and B. A. Barsky. An intuitive approach to geometric continuity for parametric curves and surfaces. In M. Wein and E. M. Kidd, editors, *Graphics Interface '85 Proceedings*, pages 343–351. Canadian Inf. Process. Soc., 1985.
26. Tony D. DeRose and Brian A. Barsky. Geometric continuity, shape parameters, and geometric constructions for catmull-rom splines. *ACM Transactions on Graphics*, 7(1):1–41, January 1988.
27. W.-H. Du and F. J. M. Schmitt. New results for the smooth connection between tensor

product bezier patches. In N. Magnenat-Thalmann and D. Thalmann, editors, *New Trends in Computer Graphics (Proceedings of CG International '88)*, pages 351–363. Springer-Verlag, 1988.

28. W.-H. Du and J.M. Schmitt. g^1 smooth connection between rectangular and triangular bézier patches at a common corner. In P. J. Laurent, A. LeMéhauté, and L. L. Schumaker, editors, *Curves and Surfaces*, pages 165–168. Academic Press, 1991.
29. W.-H. Du and J.M. Schmitt. On the g^2 continuity of piecewise parametric surfaces. In T. Lyche and L. Schumaker, editors, *Mathematical Methods in Computer Aided Geometric Design*, pages 197–207. Academic Press, 1991.
30. Nira Dyn and Charles A. Micchelli. Piecewise polynomial spaces and geometric continuity of curves. *Numer. Math.*, 54(3):319–337, 1988.
31. Gerald Farin. Smooth interpolation to scattered 3D data. In Robert E. Barnhill and Wolfgang Boehm, editors, *Surfaces in Computer-Aided Geometric Design*, pages 43–63. North-Holland, 1983.
32. Gerald Farin. Triangular Bernstein–Bézier patches. *Computer Aided Geometric Design*, 3(2):83–127, 1986.
33. I. D. Faux and M. J. Pratt. *Computational Geometry for Design and Manufacture*. Ellis Horwood, Chichester, 1979.
34. Helaman Ferguson, Alyn Rockwood, and Jordan Cox. Topological design of sculptured surfaces. In Edwin E. Catmull, editor, *Computer Graphics (SIGGRAPH '92 Proceedings)*, volume 26,2, pages 149–156, July 1992.
35. T. Garrity and J. Warren. Geometric continuity. *Computer Aided Geometric Design*, 8(1):51–66, February 1991.
36. T. Goodman. Closed surfaces defined from biquadratic splines. *Constructive Approximation*, 7(2):149–160, 1991.
37. T. N. T. Goodman. Construction piecewise rational curves with frenet frame continuity. *Computer Aided Geometric Design*, 7(1-4):15–31, June 1990.
38. T. N. T. Goodman. Joining rational curves smoothly. *Computer Aided Geometric Design*, 8(6):443–464, December 1991.
39. W. Gordon. Free-form surface interpolation through curve networks. Technical Report GMR-921, General Motors Research Laboratories, 1969.
40. W. Gordon. Spline-blended surface interpolation through curve networks. *J of Math and Mechanics*, 18(10):931–952, 1969.
41. J. Gregory. Geometric continuity. In T. Lyche and L. Schumaker, editors, *Mathematical Methods in Computer Aided Geometric Design*, pages 353–372. Academic Press, 1989.
42. J. A. Gregory. *Smooth interpolation without twist constraints*, pages 71–88. Academic Press, 1974.
43. J. A. Gregory and K. H. Lau. High order continuous polygonal patches. In G. Farin, H. Hagen, H. Noltemeier, and W. Knödel, editors, *Geometric modelling*, volume 8 of *Computing. Supplementum*, pages 117–132, Wien / New York, 1993. Springer.
44. J. A. Gregory, V. K. H. Lau, and J. M. Hahn. High order continuous polygonal patches. In *Geometric modelling*, pages 117–132. Springer, Vienna, 1993.
45. John A. Gregory and Jörg M. Hahn. Geometric continuity and convex combination patches. *Comput. Aided Geom. Design*, 4(1-2):79–89, 1987. Special issue on topics in computer aided geometric design (Wolfenbüttel, 1986).

46. John A. Gregory and Jorg M. Hahn. A C^2 polygonal surface patch. *Computer Aided Geometric Design*, 6(1):69–75, 1989.
47. John A. Gregory and Jianwei Zhou. Filling polygonal holes with bicubic patches. *Computer Aided Geometric Design*, 11(4):391–410, 1994.
48. John A. Gregory and Jianwei Zhou. Irregular C^2 surface construction using bi-polynomial rectangular patches. *Comput. Aided Geom. Design*, 16(5):423–435, 1999.
49. C. M. Grimm and J. F. Hughes. Modeling surfaces of arbitrary topology using manifolds. *Computer Graphics*, 29(Annual Conference Series):359–368, 1995.
50. H. Hagen. Bézier-curves with curvature and torsion continuity. *Rocky Mtn. J of Math.*, 16(3):629–638, 1986.
51. J. Hahn. Filling polygonal holes with rectangular patches. 1988. Blaubeuren, Germany.
52. Jorg M. Hahn. Geometric continuous patch complexes. *Computer Aided Geometric Design*, 6(1):55–67, 1989.
53. T. Hermann. G^2 interpolation of free-form curve networks by biquintic Gregory patches. *Comput. Aided Geom. Design*, 13:873–893, 1996.
54. Thomas Hermann and Gábor Lukács. A new insight into the G^n continuity of polynomial surfaces. *Computer Aided Geometric Design*, 13(8):697–707, 1996.
55. Thomas Hermann, Gábor Lukács, and Franz-Erich Wolter. Geometrical criteria on the higher order smoothness of composite surfaces. *Comput. Aided Geom. Design*, 16(9):907–911, 1999.
56. G. Herron. Smooth closed surfaces with discrete triangular interpolants. *Computer Aided Geometric Design*, 2(4):297–306, 1985.
57. G. Herron. *Techniques for visual continuity*, pages 163–174. SIAM, 1987.
58. Morris W. Hirsch. *Differential topology*. Springer-Verlag, New York, 1994. Corrected reprint of the 1976 original.
59. K. Höllig and J. Koch. Geometric hermite interpolation. *Computer Aided Geometric Design*, 12(6):567–580, 1995. ISSN 0167-8396.
60. K. Höllig and J. Koch. Geometric hermite interpolation with maximal order and smoothness. *Computer Aided Geometric Design*, 13(8):681–695, 1996. ISSN 0167-8396.
61. K. Höllig and H. Mögerle. G-splines. *Computer Aided Geometric Design*, 7(1–4):197–207, June 1990.
62. Klaus Höllig. Geometric continuity of spline curves and surfaces. TR 645, Computer Sciences Department, University of Wisconsin, Madison, WI, June 1986.
63. Klaus Höllig. Algorithms for rational spline curves. In *Transactions of the Fifth Army Conference on Applied Mathematics and Computing (West Point, NY, 1987)*, pages 287–300. U.S. Army Res. Office, Research Triangle Park, NC, 1988.
64. Klaus Höllig and Harald Mögerle. G-splines. *Comput. Aided Geom. Design*, 7(1-4):197–207, 1990. Curves and surfaces in CAGD '89 (Oberwolfach, 1989).
65. J. Hoschek. Free-form curves and free-form surfaces. *Computer Aided Geometric Design*, 10(3):173–174, August 1993.
66. Kahmann J. *Continuity of curvature between adjacent Bézier patches*, pages 65–75. North-Holland Publishing Company, Amsterdam, 1983.
67. T. Jensen. Assembling triangular and rectangular patches and multivariate splines. In G. Farin, editor, *Geometric Modeling: Algorithms and New Trends*, pages 203–220. SIAM, Philadelphia, 1987.

68. T. W. Jensen, C. S. Petersen, and M. A. Watkins. Practical curves and surfaces for a geometric modeler. *Computer Aided Geometric Design*, 8(5):357–370, November 1991.
69. A.K. Jones. Nonrectangular surface patches with curvature continuity. *Comput. Aided Design*, 20(6):325–, 1988.
70. B. Jüttler and P. Wassum. Some remarks on geometric continuity of rational surface patches. *Computer Aided Geometric Design*, 9(2):143–158, June 1992.
71. Jinggong Li, Josef Hoschek, and Erich Hartmann. G^{n-1}-functional splines for interpolation and approximation of curves, surfaces and solids. *Computer Aided Geometric Design*, 7(1-4):209–220, June 1990.
72. D. Liu and J. Hoschek. GC^1 continuity conditions between adjacent rectangular and triangular Bézier surface patches. *Computer Aided Design*, 21(4):194–200, 1989.
73. Ding-yuan Liu. A geometric condition for smoothness between adjacent bézier surface patches. *Acta Mathematicae Applicatae Sinica*, 9(4), 1986.
74. J. Manning. Continuity conditions for spline curves. *The Computer J*, 17(2):181–186, 1974.
75. T. Müller and H. Prautzsch. *A free form spline software package*. Universität Karlsruhe, 1996.
76. M. Neamtu and P. R. Pfluger. Degenerate polynomial patches of degree 4 and 5 used for geometrically smooth interpolation in R^3. *Computer Aided Geometric Design*, 11(4):451–474, 1994.
77. G. Nielson. *Some Piecewise Polynomial Alternatives to Splines Under Tension*, pages 209–235. Academic Press, 1974.
78. J. Pegna and F. Wolter. Geometric criteria to guarantee curvature continuity of blend surfaces. *ASME Transactions, J. of Mech. Design*, 114, 1992.
79. J. Peters. Local cubic and bicubic C^1 surface interpolation with linearly varying boundary normal. *Computer-Aided Geometric Design*, 7:499–515, 1990.
80. J. Peters. Smooth mesh interpolation with cubic patches. *Computer Aided Design*, 22(2):109–120, 1990.
81. J. Peters. Parametrizing singularly to enclose vertices by a smooth parametric surface. In S. MacKay and E. M. Kidd, editors, *Graphics Interface '91, Calgary, Alberta, 3–7 June 1991: proceedings*, pages 1–7, 243 College St, 5th Floor, Toronto, Ontario M5T 2Y1, Canada, 1991. Canadian Information Processing Society.
82. J. Peters. Smooth interpolation of a mesh of curves. *Constructive Approximation*, 7:221–247, 1991. Winner of SIAM Student Paper Competition 1989.
83. J. Peters. Joining smooth patches at a vertex to form a C^k surface. *Computer-Aided Geometric Design*, 9:387–411, 1992.
84. J. Peters. Surfaces of arbitrary topology constructed from biquadratics and bicubics. In Nickolas S. Sapidis, editor, *Designing fair curves and surfaces: shape quality in geometric modeling and computer-aided design*, pages 277–293. Society for Industrial and Applied Mathematics, Philadelphia, PA, USA, 1994.
85. J. Peters. C^1-surface splines. *SIAM Journal on Numerical Analysis*, 32(2):645–666, 1995.
86. J. Peters. Curvature continuous surfacing, 1998. presentation at the Oberwolfach seminar on Curves and Surfaces.
87. J. Peters. Curvature continuous free-form surfaces of degree 5,3. *Computer-Aided Geometric Design*, x(x):xx–xx, 200x. submitted.

88. J. Peters and L. Kobbelt. The platonic spheroids. Technical Report 97-052, Dept of Computer Sciences, Purdue University, 1998.
89. J. Peters and U. Reif. The 42 equivalence classes of quadratic surfaces in affine n-space. *Computer-Aided Geometric Design*, 15:459–473, 1998.
90. J. Peters and U. Reif. Analysis of generalized B-spline subdivision algorithms. *SIAM Journal on Numerical Analysis*, 35(2):728–748, April 1998.
91. J. Peters and G. Umlauf. Gaussian and mean curvature of subdivision surfaces. In R. Cipolla and R. Martin, editors, *The Mathematics of Surfaces IX*, pages 59–69. Springer, 2000.
92. Bruce R. Piper. Visually smooth interpolation with triangular Bézier patches. In Gerald Farin, editor, *Geometric Modeling : Algorithms and New Trends*, pages 221–233, Philadelphia, 1987. SIAM.
93. H. Pottmann. A projectively invariant characterization of G^2 continuity for rational curves. In G. Farin, editor, *NURBS for Curve and Surface Design*, pages 141–148. SIAM, Philadelphia, 1991.
94. Helmut Pottmann. Projectively invariant classes of geometric continuity for CAGD. *Computer Aided Geometric Design*, 6(4):307–321, 1989.
95. H. Prautzsch. Freeform splines. *Comput. Aided Geom. Design*, 14(3):201–206, 1997.
96. H. Prautzsch and G. Umlauf. Triangular G^2splines. In L.L. Schumaker P.J. Laurent, A. LeMéhauté, editor, *Curve and Surface Design*, pages 335–342. Vanderbilt University Press, 2000.
97. Abedallah Rababah. High order approximation method for curves,. *Computer Aided Geometric Design*, 12(1):89–102, 1995.
98. U. Reif. TURBS—topologically unrestricted rational B-splines. *Constr. Approx.*, 14(1):57–77, 1998.
99. Ulrich Reif. Biquadratic G-spline surfaces. *Computer Aided Geometric Design*, 12(2):193–205, 1995.
100. Ulrich Reif. *Analyse und Konstruktion von Subdivisionsalgorithmen für Freiformflächen beliebiger Topologie*. Shaker Verlag, Aachen, 1999.
101. G. Renner. Polynomial n-sided patches. *Curves and Surfaces*, pages xx–xx, 1990.
102. Walter Rudin. *Principles of Mathematical Analysis*. McGraw-Hill, Tokio, 3 edition, 1976.
103. M. Sabin. Conditions for continuity of surface normals between adjacent parametric surfaces. Technical Report VTO/MS/151, British Aircraft Corporation, 1968.
104. M. Sabin. Parametric splines in tension. Technical Report VTO/MS/160, British Aircraft Corporation, 1970.
105. M.A. Sabin. Conditions for continuity of surface normal between adjacent parametric surfaces. Technical Report VTO/MS/151, Tech. Rep., British Aircraft Corporation Ltd., 1968.
106. Malcolm A. Sabin. *The use of Piecewise Forms for the numerical representation of shape*. PhD thesis, Computer and Automation Institute, 1977.
107. R. Sarraga. G^1 interpolation of generally unrestricted cubic Bézier curves. *Computer Aided Geometric Design*, 4(1-2):23–40, 1987.
108. R. Sarraga. Errata: G^1 interpolation of generally unrestricted cubic Bézier curves. *Computer Aided Geometric Design*, 6(2):167–172, 1989.
109. H.-P. Seidel. Geometric constructions and knot insertion for geometrically continuous spline curves of arbitrary degree. Technical Report 90-024, Dept of Computer Sciences,

University of Waterloo, 1990.

110. Hans-Peter Seidel. New Algorithms and Techniques for Computing With Geometrically Continuos Spline Curves of Arbitrary Degree. *Modélisation mathématique et Analyse numérique (M^2AN)*, 26:149–176, 1992.

111. Hans-Peter Seidel. Polar Forms for Geometrically Continous Spline Curves of Arbitrary Degree. *ACM Transactions on Graphics*, 12(1):1–34, January 1993.

112. L. A. Shirman and C. H. Séquin. Local surface interpolation with Bézier patches: Errata and improvements. *Computer Aided Geometric Design*, 8(3):217–222, August 1991.

113. Leon A. Shirman. *Construction of smooth curves and surfaces from polyhedral models*. Ph.d. thesis, Computer Science Division (EECS), University of California, Berkeley, 1990.

114. Leon A. Shirman and Carlo H. Sequin. Local surface interpolation with bezier patches. *Computer Aided Geometric Design*, 4(4):279–295, December 1987.

115. J. van Wijk. Bicubic patches for approximating non-rectangular control-point meshes. *Computer Aided Geometric Design*, 3(1):1–13, 1986.

116. M. Veron, R. Riss, and J.-P. Musse. Continuity of biparametric surface patches. *Computer-Aided Design*, 8:267–273, October 1976.

117. A. Vinacua and P. Brunet. A construction for VC^1 continuity for rational Bézier patches. In T. Lyche and L. Schumaker, editors, *Mathematical Methods in Computer Aided Geometric Design*, pages 601–611. Academic Press, 1989.

118. Du W.-H. *Etude sur la représentation d surfaces complexes: application à la reconstruction de surfaces échantillonnes*. PhD thesis, Ecole National Supérieure des télé–communications, October 1988.

119. Wallner and H. Pottmann. Orbifolds. In *xxx*, pages –, 1998.

120. J. Warren. Blending algebraic surfaces. *ACM Transactions on Graphics*, 8(4):263–278, October 1989.

121. Joe D. Warren. On algebraic surfaces meeting with geometric continuity. Technical Report TR86-770, Cornell University, Computer Science Department, August 1986.

122. P. Wassum. *Bedingungen und Konstruktione zur geometrischen Stetigkeit und Anwendungen auf approximative Basistransformationen*. PhD thesis, TH Darmstadt, 1991.

123. P. Wassum. Geometric continuity between adjacent rational Bézier surface patches. In G. Farin, H. Hagen, H. Noltemeier, and W. Knödel, editors, *Geometric modelling*, volume 8 of *Computing. Supplementum*, pages 291–316, Wien/New York, 1993. Springer.

124. M. Watkins. Problems in geometric continuity. *Computer Aided Design*, 20(8):499–502, 1988.

125. Jörg Weber. Constructing a boolean-sum curvature-continuous surface. In F.-L. Krause and H. Jansen, editors, *Advanced geometric modleing for engineering applications*, pages 103–116, 19xx.

126. F. Yamaguchi. *Curves and Surfaces in Computer-Aided Geometric Design*. Springer, Berlin, 1988.

127. Xiuzi Ye. Curvature continuous interpolation of curve meshes. *Computer Aided Geometric Design*, 14(2):169–190, 1997.